This is the author's accepted manuscript of the article published in The Journal of Allergy and Clinical Immunology. The final authenticated version is available online at: https://doi.org/10.1016/j.jaci.2023.02.026

A20 is a master switch of IL-33 signalling in macrophages and determines IL-33-induced lung immunity

Aurora Holgado MSc[1,2], Zhuangzhuang Liu MSc[2,3], Aigerim Aidarova MSc[1,2], Christina Mueller PhD[1,2], Mira Haegman BSc[1,2], Yasmine Driege BSc[1,2], Marja Kreike BSc[1,2], Charlotte L. Scott PhD[2,3], Inna S. Afonina PhD[1,2*] and Rudi Beyaert PhD[1,2*]

[1]Unit of Molecular Signal Transduction in Inflammation, VIB-UGent Center for Inflammation Research, Ghent, Belgium.

[2]Department of Biomedical Molecular Biology, Ghent University, Ghent, Belgium.

[3]Laboratory of Myeloid Cell Biology in Tissue Damage and Inflammation, VIB-UGent Center for Inflammation Research, Ghent, Belgium.

[*]These authors share senior authorship.

Corresponding author: Rudi Beyaert, PhD, Unit of Molecular Signal Transduction in Inflammation, VIB-UGent Center for Inflammation Research, Ghent, Belgium. E-mail: Rudi.Beyaert@irc.vib-ugent.be

Funding sources: Research in the authors' lab is supported by grants from the VIB Grand Challenges Program (GC01-C01), the Fund for Scientific Research Flanders (FWO) Excellence of Science (EOS) research programme (3G0I1422), Ghent University Concerted Research Actions (GOA; 01G00419). I.S.A. holds a fundamental mandate of the Foundation against Cancer. Z.L. is funded by a Chinese Scholarship Council Grant.

The authors declare that they have no conflicts of interest.

Word Count: 6495

Abstract

Background: IL-33 plays a major role in the pathogenesis of allergic diseases such as asthma and atopic dermatitis. Upon its release from lung epithelial cells, IL-33 primarily drives type 2 immune responses, accompanied by eosinophilia and robust production of IL-4, IL-5 and IL-13. However, several studies show that IL-33 can also drive a type 1 immune response.

Objective: Important questions remain regarding the mechanisms that determine whether IL-33 induces a type 1 or type 2 immune response. Here we focus on the role of A20 in the regulation of IL-33 signalling in macrophages and IL-33-induced lung immunity.

Methods: We studied the immunological response in lungs of IL-33-treated mice that specifically lack A20 in myeloid cells. We also analysed IL-33 signalling in A20-deficient bone marrow derived macrophages.

Results: IL-33-induced lung ILC2 expansion, type 2 cytokine production and eosinophilia was drastically reduced in the absence of macrophage A20 expression, while neutrophils and interstitial macrophages in lung were increased. In vitro, IL-33-mediated NF-κB activation was only weakly affected in A20-deficient macrophages. However, in the absence of A20, IL-33 gained the ability to activate STAT1 signalling and STAT1-dependent gene expression. Surprisingly, A20-deficient macrophages produced IFN-γ in response to IL-33, which was fully STAT1-dependent. Furthermore, STAT1 deficiency partially restored the ability of IL-33 to induce ILC2 expansion and eosinophilia in myeloid cell-specific *A20* knockout mice.

Conclusion: We reveal a novel role for A20 as a negative regulator of IL-33-induced STAT1 signalling and IFN-γ production in macrophages, which determines lung immune

responses.

Clinical implications: Our findings may eventually help to identify strategies that allow a better stratification of patients, leading to enhanced treatment efficacy.

Capsule summary:

A20 deficiency in macrophages prevents IL-33-induced type 2 immune responses in the lung, which may have important implications in IL-33 mediated diseases such as asthma and atopic dermatitis.

Key words: IL-33; TNFAIP3; macrophages; mouse models, interferon-γ; airway inflammation; eosinophilia, allergic asthma, autoimmunity.

Abbreviations: AM alveolar macrophages; BAL bronchoalveolar lavage; BMDM bone marrow-derived macrophages; DC dendritic cell; HDM house dust mite; IFN-γ interferon gamma; **I**L-33 Interleukin-33; IL-1RAcP IL-1 receptor accessory protein; ILC2 Innate lymphoid cells type 2; IMs interstitial macrophages; i.t. intratracheal; MAPK mitogen-activated protein kinase; NF-κB nuclear factor-kappa B; NOS nitric oxide synthase; qRT-PCR quantitative real-time PCR; Relmα resistin-like molecule α; TNF tumour necrosis factor; TF transcription factor.

Introduction

Asthma is a heterogeneous chronic inflammatory disease of the respiratory system, caused by an aberrant response of the immune system to environmental insults such as allergens or pollutants which predominantly triggers a type 2 cytokine-driven eosinophilic airway inflammation ultimately resulting in airway hyperresponsiveness, mucus overproduction, as well as remodelling and narrowing of airway walls. However, one third of patients with severe asthma are suffering from a so-called type 2-low endotype, defined by the absence of signature type 2 cytokines and eosinophil infiltration, and sometimes include severe disease cases predominantly controlled by the presence of neutrophils and a mix of type 1/type 17 cytokines[1]. Unlike eosinophilic asthma, type 2-low asthma patients respond poorly to inhaled corticosteroids[2]. Despite presenting a significant clinical challenge, the molecular mechanisms responsible for type 2-low asthma are still poorly characterised. Recently, the intracellular protein A20, also known as tumour necrosis factor α-induced protein 3 (TNFAIP3), has been implicated as a gatekeeper against neutrophilic airway inflammation[3,4].

A20 is a potent anti-inflammatory protein, and defects in A20 activity have been associated with several inflammatory pathologies including asthma[5]. Polymorphisms in the *A20* locus are associated with risk of asthma and allergies in humans, and cell-type specific deletion of A20 in mice was shown to sensitize to allergic lung inflammation[6–8]. Reduced A20 expression was found in peripheral blood mononuclear cells from asthmatic children compared to healthy controls, and also in newborns who subsequently suffer from asthma at school age[9]. Moreover, airway epithelial cells from adult asthmatics were shown to produce significantly less A20 than cells from healthy patients[6]. Although the

precise role of A20 in asthma development and progression remains incompletely understood, studies with cell-type specific *A20* knockout mice support an important role of A20 expression in lung stromal cells as well as immune cells. In this regard, specific deletion of *A20* in lung epithelial cells or mast cells increases the sensitivity of mice to house-dust mite (HDM)-induced allergic airway inflammation[6,10]. On the other hand, mice lacking A20 in myeloid cells develop neutrophilic airway inflammation in response to HDM exposure rather than the classical HDM-induced lung eosinophilia[3,11]. Mechanistically, ablation of A20 in pulmonary dendritic cells (DCs) leads to increased DC activation, and their subsequent production of cytokines, expression of costimulatory molecules and DC-mediated activation of auto-reactive T- and B-cell responses[3,4,11,12].

While an important role of A20 in the regulation of lung inflammation is now well accepted, the key receptors and downstream signalling pathways that are negatively regulated by A20 and induce a non-eosinophilic type 2-low allergic response when A20 is defective, remain to be determined. IL-33 is a key cytokine whose release from airway epithelial cells upon allergen exposure initiates a type 2 inflammatory response through the activation of innate lymphoid cells type 2 (ILC2s) and $CD4^+$ T cells[13]. However, several other cell types such as eosinophils, basophils, mast cells, and macrophages can also respond directly to IL-33 and contribute to an allergic response[14]. Single-nucleotide polymorphisms identified in the genomic region of both IL-33 and the IL-33 receptor ST2 are associated with susceptibility to asthma development and increased disease severity[15–17]. Moreover, increased IL-33 levels in the bronchial lavage, sputum and serum of patients with asthma correlates with disease exacerbations[18–20], while IL-33 expression in bronchial biopsies is also associated with airway hyperresponsiveness[21]. Blockade of

IL-33 signalling has been shown to suppress allergic airway inflammation in murine models[22–28], and monoclonal antibodies neutralizing IL-33 activity are actively developed as new therapeutics in asthma and other atopic diseases in humans[29]. Extracellular IL-33 exerts its activities by triggering nuclear factor-kappa B (NF-κB) and mitogen-activated protein kinase (MAPK) signalling pathways that control the expression of pro-inflammatory genes[30]. A20 has been almost exclusively studied in the context of its ability to inhibit TNF-, IL-1- and TLR-induced NF-κB signalling in different cell types[5], but little is known about its effect on the response to other cytokines such as IL-33. Only IL-33-induced mast cell activation was shown to be inhibited by A20[10]. Because macrophages are the most prominent immune cells normally residing on the respiratory mucosal surface and are capable of either promoting or suppressing inflammatory responses in the airway, we sought to investigate whether A20 controls immune responses in the lung via the regulation of IL-33 signalling in macrophages. Therefore, we made use of previously described A20 $^{LysM\text{-}KO}$ mice that lack A20 in macrophages[31].

Materials and Methods

Antibodies, expression plasmids, and other reagents

Detailed information regarding antibodies used for the flow cytometry experiments (including antibody dilution, manufacturer, catalogue number) is listed in Table E1 in the Online Repository.

The following antibodies were used for western blotting: anti-phospho-JNK1/2 polyclonal antibodies (446826G, Invitrogen and 4668, Cell Signalling Technology), anti-JNK1/2 monoclonal antibody (554285, BD Biosciences), anti-p38 MAPK polyclonal antibody (9212, Cell Signaling Technology), anti-phospho-p38 MAPK (Thr180/Tyr182) monoclonal antibody (9215, Cell Signaling Technology), anti-IκBα polyclonal antibody (sc-371, Santa Cruz), anti-phospho-IκBα (Ser32/36) (9246, Cell Signaling Technology), anti-actin monoclonal antibody (MP6472J, MP Biomedicals), anti-A20 monoclonal antibody (sc-52910 or sc-166692, Santa Cruz), anti-phospho-STAT1 polyclonal antibody (9167, Cell Signalling Technology), anti-STAT1 monoclonal antibody (sc-271661, Santa Cruz), anti-phospho-STAT6 polyclonal antibody (56554, Cell Signalling Technology), anti-STAT6 monoclonal antibody (sc-374021, Santa Cruz). HRP-conjugated goat anti-mouse IgG cross-adsorbed secondary antibody (31432) or mouse anti-rabbit IgG cross-adsorbed secondary antibody (31464) were from Invitrogen (ThermoFisher Scientific).

ELISA sets for human IL-8 (88-8086-88) and mouse IL-4 (88-7044-88), IL-5 (88-7054-77), IL-13 (88-7137-88), IL-17A (88-7371-88), IFN-γ (88-7314-77) were from eBioscience (ThermoFisher Scientific). Plasmids have been deposited at the BCCM-GeneCorner plasmid collection (Ghent, Belgium), and accession numbers are provided for each

plasmid. pNFconluc (LMBP3248), which contains NF-κB-driven luciferase (LMBP3248), was a gift from Dr. A. Israël (Institut Pasteur, Paris, France), and pACTβgal (LMBP4341) was from Dr. J. Inoue (Institute of Medical Sciences, Tokyo, Japan).

Cell culture and bioassays

HEK 293T cells (human embryonic kidney cells) were cultured in Dulbecco modified Eagle medium (Gibco) supplemented with 10% FCS and 2 mM L-glutamine. HEK 293T cells were a gift from Dr. Hall (Department of Biochemistry, University of Birmingham, United Kingdom). For the IL-33 bioassay, HEK 293T cells were seeded at 4 X 10^4 cells/well in 24-well plates and transiently transfected the next day using calcium phosphate precipitation method with IL-33 receptor subunits plasmids (pEF-BOS-hST2 (kindly provided by Professor Luke O'Neill (Trinity College, Dublin, Ireland), LMBP13244) and pEF6-IL-1RAcP (LMBP07863)). Cells were co-transfected with the NF-κB reporter plasmid pNFconluc and the constitutively expressing β-galactosidase plasmid pACTbgal, as well as A20 expression constructs (pCAGGS-hA20 (LMBP03778), pCAGGS-hA20(C624A–C627A) (ZF4_Mut; LMBP06563), pCAGGS-hA20(C775A–C779A) (ZF7_Mut; LMBP06569), pCAGGS-hA20(C624A–C627A/C775A–C779A) (ZF4/7_Mut; LMBP06570), and pCAGGS-hA20(D100A/C103A) (DUB_Mut; LMBP06056)). 24 h later, cells were stimulated with recombinant IL-33 for 5 h. Luciferase activity was measured in cell lysates 5 hours later and normalized based on β-galactosidase values to correct for potential differences in transfection efficiency. Cytokine profiles in cell supernatants were measured 24 hours later using an ELISA, according to the manufacturer's protocol.

For the generation of bone marrow-derived macrophages (BMDMs), bone marrow cells

obtained from tibiae and femurs of A20 $^{LysM-KO}$ and A20 $^{LysM-WT}$ mice were cultured for 6 days in RPMI 1640 (Gibco) supplemented with 10% FCS (Bodinco), 1% GlutaMAX (Gibco), 100 IU/ml penicillin, 100 µg/ml streptomycin, 50 µM β-mercaptoethanol (all from ThermoFisher Scientific) and 40 ng/ml recombinant mouse M-CSF (VIB Protein Core facility). BMDMs were of ≥95% purity as measured by flow cytometry using F4/80 and CD11b specific antibodies. Cells were plated at 7 X 10^5 cells per well in 6 well plates and pre-stimulated with 10 ng/ml mouse recombinant IL-4 (12340045, Immunotools) for 18 h, followed for the indicated times by stimulation with 100 ng/ml mouse recombinant IL-33 that was pre-incubated (15 min) or not with 1000 ng/ml IL-33trap inhibitor (produced as described previously[28]). Gene and protein expression were analysed by quantitative real-time PCR (qRT-PCR) or western blot, respectively. The activity of the 48 transcription factors in the nuclear extracts of IL-4 and IL-33 stimulated cells (5 µg) was analysed according to the manufacturer's instructions (Signosis, FA-1001).

In vivo IL-33-induced airway inflammation

Generation of A20$^{fl/fl}$ LysM-Cre transgenic mice is described in detail in [31]. All experiments on mice were performed according to institutional (Ethical Committee for Animal Experimentation at Ghent University's Faculty of Sciences), national and European animal regulations. Mice were housed in individually ventilated cages at the VIB-UGent Center for Inflammation Research in specific pathogen-free animal facility.

For the treatment of animals with IL-33, mice were anesthetized with isoflurane and received 1 µg of recombinant mouse IL-33 or PBS administered intratracheally (i.t.) every day for 5 days. The dose was chosen based on previous studies[28,32,33]. Mice were

sacrificed on day 6 and bronchoalveolar lavage (BAL) fluid, as well as lungs were collected for further analysis. BAL was performed with 3 X 1 mL of EDTA-containing PBS via a cannula inserted in the trachea and analysed by using flow cytometry.

Lungs were cut into small pieces and incubated at 37°C for 30 minutes in RPMI 1640 containing 40 μg/ml Liberase TM (Roche, Mannheim, Germany) and 10 U/ml DNase I (Roche). Lungs were filtered over a 70-μm strainer (Falcon), and red blood cells were lysed with 1 mL of ACK lysis buffer (Lonza) for 3 minutes on ice before staining with different fluorescence-activated cell sorting antibodies.

Lungs were snap-frozen in liquid nitrogen and kept at -80°C until further processing for q RT-PCR or cytokine measurement by means of ELISA.

Flow cytometry

Cell suspensions from BAL fluid and lung tissue were quantified by using flow cytometry. Unspecific antibody binding was prevented by adding 2.4G2 (antibody to the Fcγ receptor II/III (553142, BD Biosciences)) during the staining. Dead cells were excluded from the analysis by using fixable viability dye eFluor506 or eFluor 780 (eBioscience), and 123count Beads (Invitrogen) were used to determine absolute cell numbers. The antibodies used and corresponding information are listed in Table E1 in the Online Repository. Multiparameter analysis was performed on an LSRFortessa (BD), and data were processed with FlowJo software (TreeStar, Ashland, Ore). Cell sorting was performed on FACSymphony™ S6 Cell Sorter (BD). Representative gating strategies are shown in Figures E1 and E2 in the Online Repository.

Cytokines quantification

Lungs were homogenized with a tissue homogenizer in 320 μL of cold lysis buffer (40 mM Tris-HCl [pH 8.0], 0.275 mM NaCl, 20% glycerol [vol/vol], 1 mM phenylmethylsulfonyl fluoride, 1 mM sodium orthovanadate [Na3VO4], 10 mM NaF, 1 μg/mL aprotinin, and 1 μg/mL leupeptin) by using a tissue homogenizer (IKA, Wilmington, NC) with addition of 2% Igepal after homogenization. Samples were then rotated for 20 minutes at 4°C with agitation, followed by centrifugation to pellet debris. Cleared lysate was quantified for protein concentration by using the Bradford Bio-Rad protein assay (Bio-Rad Laboratories). Concentrations of cytokines and chemokines in whole-lung homogenates, BAL fluid and cell cultures supernatant were measured by ELISA, according to the manufacturer's protocol.

RNA isolation, cDNA synthesis and qRT-PCR

RNA from lung tissue and BMDMs lysates was obtained by using the TriPure Isolation Reagent (Roche) and isolated according to the manufacturer's instructions. The purity of RNA was determined by analysing OD260/280 ratio (for RNA approx. 2.0) and OD260/230 ratio (2.0-2.2). RNA was reverse transcribed with an iScript Advanced cDNA Synthesis Kit (Bio-Rad Laboratories), and samples were analyzed by using SYBR green−based qRT-PCR with a LightCycler 480 system (Roche). Analysis was done using qBase^{+} software (Biogazelle). Results are presented as relative expression values that were normalized to the appropriate amount of reference genes, as determined by geNorm analysis in the qBase^{+} software. Relative quantification thus determines the changes in

steady-state mRNA levels of a gene across multiple samples and expresses it relative to the levels of an internal control RNA that is used as reference gene.

The following mouse gene-specific primers were used (5'–3'):

*Actb*F,GCTTCTAGGCGGACTGTTACTGA; *Actb*R GCCATGCCAATGTTGTCTCTTAT;

*Acod1*F TGGTGTTGCTGTTCACTCCA; *Acod1*R TCGGGGGAGTAGTTGGCATA;

*Arg1*F AAGAAACAGAGTATGACGTGAG; *Arg1*R GAGTGTTGATGTCAGTGTGAG;

*Ccl24*F ATTCTGTGACCATCCCCTCAT; *Ccl24*R TGTATGTGCCTCTGAACCCAC;

*Cxcl1*F GAGCCTCTAACCAGTTCCAG; *Cxcl9*R TGAGTGTGGCTATGACTTCG

*Hprt1*F AGTGTTGGATACAGGCCAGAC; *Hprt1*R CGTGATTCAAATCCCTGAAGT;

*Ifit1*F CTACCACCTTTACAGCAACC; *Ifit1*R AGATTCTCACTTCCAAATCAGG;

*Ifng*F CTGCTGATGGGAGGAGATGT; *Ifng* R TTTGTCATTCGGGTGTAGTCA;

*Il1b*F CACCTCACAAGCAGAGCACAAG; *Il1b*R GCATTAGAAACAGTCCAGCCCATAC;

Il5F CTCTGTTGACAAGCAATGAGACG; *Il5R* TCTTCAGTATGTCTAGCCCCTG;

*Il6*F GAGGATACCACTCCCAACAGACC; *Il6*R AAGTGCATCATCGTTGTTCATACA;

Il13F TCAGCCATGAAATAACTTATTGTTTTGT; *Il13R* CCTTGAGTGTAACAGGCCATTCT;

*Nos2*F CAGCTGGGCTGTACAAACCTT; *Nos2*R CATTGGAAGTGAAGCGTTTCG;

*Retnla*F CCAATCCAGCTAACTATCCCTCC; *Retnla*R ACCCAGTAGCAGTCATCCCA;

*Rpl13a*F CCTGCTGCTCTCAAGGTT; *Rpl13a*R TGGTTGTCACTGCCTGGTACTT;

*Tbp*F TCTACCGTGAATCTTGGCTGTAAA; *Tbp*R TTCTCATGATGACTGCAGCAAA;

Tissue sample preparation and histology.

Lungs were collected and fixed in 4% PFA in PBS at 4°C overnight, dehydrated, embedded in paraffin and sectioned. Sections of 5 µm were deparaffinized followed by staining with hematoxylin-eosin. For combined alcian blue (AB) and periodic acid-Schiff (PAS) staining, dewaxed sections were hydrated and incubated in AB for 5 min. Sections were subsequently washed with water before incubation in 1% periodic acid for 5 min followed by incubation in Schiff's reagent for 15 min. Sections were counterstained with Mayer's haematoxylin for 30 s, washed and dehydrated before mounting. The staining was performed in autostainer XL (Leica). Masson's trichrome staining was performed as described by the manufacturer's instructions in the Trichrome Stain (Masson) kit (HT15, Sigma). Sections were mounted by use of Entellan mounting medium (1079610100, Merck Millipore). Images were acquired with Zeiss Axio Scan Z1 Slide Scanner (Zeiss) and analyzed using ZEN software.

Statistical analyses

Results are expressed as means ± SEM. Statistical analysis was performed with GraphPad Prism software (version 9.3.1) using two-way ANOVA to determine significant differences, unless otherwise specified. Log transformation was used on the data if it failed normality test. Differences between groups were considered significant when the p-value was < 0.05.

Results

Myeloid cell A20 controls IL-33-induced immune responses in the lung

We first analysed whether A20 expression in myeloid cells controls IL-33-driven immune responses in the lung. To this end, we treated wild type mice and mice lacking A20 in myeloid cells (A20 $^{LysM-KO}$) i.t. daily with recombinant IL-33 for 5 consecutive days and assessed the presence of inflammatory cells in their BAL fluid and lung tissue. Hematoxylin and eosine staining of lung sections showed that alveolar spaces of both control (A20 $^{LysM-WT}$) mice and A20 $^{LysM-KO}$ mice were filled with large number of cells upon IL-33 treatment (Fig. 1A). Mucus production and collagen deposition were also strongly increased in response to IL-33 treatment, both in A20 $^{LysM-WT}$ and A20 $^{LysM-KO}$ mice (Fig. 1A). As expected, flow cytometry of BAL (Fig 1B) and lung tissue (Fig 1C) showed that IL-33 treatment induced a conventional type 2 immune response defined by robust eosinophilia in A20 $^{LysM-WT}$ mice. Remarkably, this IL-33-induced eosinophila was strongly reduced in BAL and lung of A20 $^{LysM-KO}$ mice.

IL-33 treatment also resulted in a significant expansion of ILC2s in the A20 $^{LysM-WT}$ lung, which was again less pronounced in A20 $^{LysM-KO}$ mice (Fig 1C). Since LysM-cre is known not to delete in ILC2s[34], the reduced numbers of ILC2s cannot be explained by defective ILC2-intrinsic IL-33 signalling and instead point to the role of myeloid cells in regulating IL-33-induced ILC2 proliferation. Neutrophil numbers in BAL fluid were increased after IL-33 treatment in both A20 $^{LysM-WT}$ and A20 $^{LysM-KO}$ mice (Fig 1B), and were drastically increased in the lung tissue of A20 $^{LysM-KO}$ mice compared to A20 $^{LysM-WT}$ (Fig 1C). A similar effect has previously been described in mice exposed to house dust mite allergen[3].

Depending on their localization, we can broadly define two well-studied populations of

lung macrophages: (1) alveolar macrophages (AMs) that populate the alveolar and airway lumen and (2) interstitial macrophages (IMs) located within the lung tissue interstitium[35]. IL-33 treatment resulted in a very strong decrease in the number of AM, which was less pronounced in A20 $^{LysM\text{-}KO}$ mice (Fig. 1B). Conversely, IL-33 treatment of wild type mice strongly increased numbers of interstitial macrophages (IMs), which was even more pronounced in the lung A20 $^{LysM\text{-}KO}$ mice (Fig. 1C). A similar increase in IMs has previously been reported in mice treated with different TLR ligands, which were shown to arise from local and splenic reservoir monocytes and have an immunosuppressive effect[36].

Cellular changes in IL-33-treated A20 $^{LysM\text{-}KO}$ mice were further accompanied by a strong decrease in the amounts of type 2 cytokines IL-4, IL-5 and IL-13 in the lung (Fig. 1D), which may also be responsible for the lowered lung eosinophilia in IL-33-treated A20 $^{LysM\text{-}KO}$ mice. No differences in IL-17 expression could be observed (Fig. 1D). To determine the source of type 2 cytokines in IL-33-treated mice, we performed qPCR for IL-5/IL-13 on different cell types isolated from lung tissue and identified $CD4^+$ T cells as the main source of *Il5* and *Il13* in IL-33-treated A20 $^{LysM\text{-}WT}$ mice (Fig. 1E). We did not detect any *Il4, Il5* or *Il13* mRNA in ILC2 cells from IL-33-treated A20 $^{LysM\text{-}WT}$ and A20 $^{LysM\text{-}KO}$ mice. Together, our results demonstrate that absence of A20 in myeloid cells drastically decreases lung eosinophil infiltration and ILC2 expansion in IL-33-treated mice, switching to a more neutrophil dominated immune response and increased numbers of IM.

The transcriptional profile and functions of macrophages are strongly influenced by the microenvironment and the local cytokine and chemokine milieu. Generally, *in vitro* stimulation of macrophages with stimuli such as IFN-γ and LPS are known to induce

expression of target genes associated with a more inflammatory phenotype (e.g. TNF, IL-1, inducible nitric oxide synthase (*Nos2*, iNOS), while in the presence of type 2 cytokines such as IL-4 and IL-13, macrophages express amongst others arginase-1 (Arg1) and resistin-like molecule (Relm)-α (*Retnla*, Relmα)[37]. During allergic airway inflammation, IL-33 has been shown to amplify IL-4/IL-13-induced macrophage activation, which in turn promotes a type 2 immune response through the secretion of cytokines and chemokines involved in inflammation, tissue repair and airway remodeling in the lung[38,39]. In agreement with previously published data, we observed that expression of *Arg1* and *Ccl24,* which are often associated with IL-4-activated macrophages, was increased in the lung tissue of IL-33-treated A20 $^{LysM\text{-}WT}$ mice, but almost completely blocked in the absence of myeloid cell-expressed A20 (Fig 2A). Instead, although independent of IL-33 treatment, the expression of proinflammatory genes (*Il1b, Cxcl1*) was higher in the lung tissue of mice that lack myeloid A20 when compared to control mice (Fig. 2A), indicating that A20-deficient macrophages are already in a slightly proinflammatory state in unstimulated conditions.

We further analysed gene expression in IMs in more detail. Importantly, expression of *Retnla* was significantly increased in IMs from IL-33-treated A20 $^{LysM\text{-}WT}$ mice, but not A20 $^{LysM\text{-}KO}$ mice (Fig. 2B). Instead IMs of A20 $^{LysM\text{-}KO}$ mice exhibited a trend towards increased expression of the proinflammatory marker *Nos2* (Fig. 2B). Collectively, these data show that in the absence of A20, lung macrophages show a drastically reduced anti-inflammatory gene expression response in IL-33-treated mice. Although at this stage we cannot exclude that some of these genes are directly induced by IL-33, their reduced expression most likely reflects decreased macrophage activation by IL-4, due to the much

lower amounts of IL-4 in the lung environment of IL-33-treated A20 $^{LysM-KO}$ mice.

Absence of A20 slightly increases IL-33-induced NF-κB activation in macrophages

A20 is known as a negative regulator of NF-κB and JNK/p38 MAPKs signalling in response to different stimuli including LPS, TNF and IL-1 family cytokines in multiple cell types[5,10]. To establish whether A20 is capable of modulating IL-33-induced NF-κB and MAPKs activation, we first analysed by western blotting if A20 overexpression in HEK293T cells is able to reduce IL-33-induced phosphorylation of IκBα, p38 and JNK, as hallmarks of NF-κB and p38/JNK MAPK activation. HEK293T cells were made IL-33-responsive by transient transfection of the IL-33 receptor ST2 and its co-receptor IL-1RAcP as described previously[28]. A20 overexpression significantly reduced IL-33-induced phosphorylation of IκBα, p38 and JNK (Fig. 3A). Similarly, overexpression of A20 strongly reduced NF-κB-dependent luciferase reporter gene expression (Fig. 3B), as well as endogenous IL-8 production (Fig. 3B) in IL-33-stimulated HEK293T cells in a dose-dependent manner. Use of different A20 mutants demonstrated that the ability of A20 to inhibit IL-33-induced NF-κB activation and IL-8 expression in HEK293T cells was dependent on its zinc finger 4 and 7 (Fig. 3C), which is in line with previous findings in the case of A20-mediated regulation of TNF-induced NF-κB activation[40].

Gene expression in macrophages is regulated *in vivo* by IL-33 and by Th2 cytokines produced by IL-33 activated ILC2s. To investigate if A20 deficiency in macrophages affects their direct response to IL-33, we studied IL-33-induced signalling and gene expression in BMDM isolated from A20 $^{LysM-}$WT and A20 $^{LysM-KO}$ mice. Importantly, BMDMs

were equally well generated from A20 $^{LysM-}$WT and A20 $^{LysM-KO}$ mice, as assessed by their expression of F4/80 and CD64 and lack of expression of Ly6G and Ly6C (see Figure E2 in the Online Repository). To investigate whether A20 also inhibits IL-33-induced NF-κB and p38/JNK activity in macrophages, we compared IL-33-induced phosphorylation of IκBα, p38 and JNK in BMDMs isolated from A20 $^{LysM-WT}$ and A20 $^{LysM-KO}$ mice (Fig. 3D). LPS-stimulated BMDMs were used as positive control[31]. WT BMDMs expressed A20 in unstimulated conditions (Fig. 3D, lane 1). As described previously, LPS treatment induced the appearance of a slower migrating A20 band due to A20 phosphorylation, which is known to increase its inhibitory capacity[41]. A similar although less pronounced effect was observed in cells treated with IL-33 for 15 min or longer. IL-33 stimulation resulted in a fast and transient increase in IκBα phosphorylation in WT cells. Unstimulated A20-deficient BMDMs already showed higher constitutive IκBα phosphorylation compared to WT cells, which was not further increased in response to IL-33. However, IκBα phosphorylation was prolonged for a longer time in IL-33-stimulated cells in the absence of A20 (Fig. 3D, compare 15 min time point). IκBα phosphorylation is known to trigger its proteasomal degradation and is later followed by the NF-κB-dependent resynthesis of IκBα. Again, IκBα resynthesis occurred slightly faster in A20-deficient cells (Fig. 3D, compare 30 min time point). We did not detect a difference in LPS-induced IκBα phosphorylation and total IκBα expression between A20 $^{LysM-WT}$ and A20 $^{LysM-KO}$ BMDMs, most likely because LPS-induced IκBα phosphorylation in both A20 $^{LysM-WT}$ and A20 $^{LysM-KO}$ cells was still at its maximum at the time points that we analysed. Together, these data illustrate that A20 slightly reduces IL-33 induced NF-κB activation in BMDMs. In contrast, absence of A20 did not have an effect on IL-33-induced p38/JNK phosphorylation (Fig.

3D), indicating that IL-33-induced MAPKs activation is insensitive to A20.

IL-33 was previously shown to induce the expression of pro-inflammatory genes (e.g. *Tnf*, *Il1b*, *Il6*) in BMDMs, followed by mitochondrial reprogramming and GATA3-dependent expression of anti-inflammatory genes (*Arg1*, *Chil3*)[42]. We next asked whether A20 regulates IL-33-induced gene expression in BMDMs. Because IL-4Ra signalling was previously shown to upregulate IL-33 receptor (ST2) expression in BMDMs, enabling IL-33-induced gene expression[39], we also pre-stimulated BMDMs with IL-4. IL-33 alone had only a minimal effect on the expression of pro-inflammatory genes (*Il1b*, *Il6* and *Cxcl1*), which is comparable in control and A20-deficient BMDMs (Fig. 3E). However, IL-33-induced responses were drastically increased in A20-deficient BMDMs if pre-stimulated with IL-4, supporting the ability of A20 to suppress IL-33-induced pro-inflammatory signalling. Importantly, addition of IL-33 inhibitor[28] abolished the expression of *Il1b*, *Il6* and *Cxcl1* in IL-4/IL-33 co-stimulated BMDMs, showing that these transcriptional responses are dependent on IL-33 signalling (Fig. 3E). In contrast, expression of *Arg*, *Ccl24* and *Retnla* was already significantly increased by IL-4 alone and did not change further upon costimulation with IL-33. Collectively, these data demonstrate that A20 negatively regulates IL-33-induced pro-inflammatory gene expression in BMDMs.

A20 deficiency sensitizes BMDMs to IL-33-induced STAT1 signalling

To better understand A20-mediated regulation of IL-33-induced gene expression in macrophages, we made use of a transcription factor (TF) array to profile the DNA-binding activity of a panel of TFs in nuclear extracts of BMDMs that were stimulated for 18 hours with IL-4, followed by the addition of IL-33 for another 24 hours. This revealed that the

activity of several TFs in response to IL-4/IL-33 co-stimulation was influenced by the presence of A20 (Fig 4A and table E2 in the Online Repository). TFs that showed at least a 4-fold increase in activity in A20 $^{LysM\text{-}KO}$ compared to A20 $^{LysM\text{-}WT}$ BMDMs are AP1, AP2, ATF2, Brn3, STAT1 and other GAS-ISRE binding TFs (Fig 4B). In contrast, STAT6 activity was strongly reduced in the absence of A20. STAT1 is well known as a TF involved in IFN-γ-induced pro-inflammatory signalling in BMDMs, while STAT6 is a major mediator of IL-4-induced anti-inflammatory signalling[43]. Therefore, we next assessed STAT1 and STAT6 expression and phosphorylation in wild type or A20-deficient BMDMs stimulated with IL-4, IL-33 or a combination of both. Consistent with previous reports STAT1 expression was strongly upregulated in A20 $^{LysM\text{-}KO}$ BMDMs but was only weakly phosphorylated[44], while STAT6 expression and phosphorylation were unaffected (Fig 4C). However, stimulation with IL-33 led to STAT1 phosphorylation in A20-deficient macrophages, which was further enhanced by IL-4 pre-treatment, illustrating specific IL-33-induced STAT1 activation. IL-4 alone was unable to induce STAT1 phosphorylation, neither in wild type nor in A20-deficient BMDMs, where STAT1 expression is increased. Furthermore, treatment of cells with an IL-33 inhibitor[28] impeded the IL-33 and IL-33 plus IL-4-induced phosphorylation of STAT1 in A20-deficient BMDMs, confirming the specificity of the IL-33 effect (Fig. 4C). The underlying mechanism by which IL-33 activates STAT1 is still unclear but may involve increased JAK kinase activation[45]. IL-33 alone did not induce STAT6 phosphorylation. On the contrary, IL-33 treatment for 24 hours, but not 3 hours, reduced IL-4-induced STAT6 phosphorylation. As this coincides with a strong IL-33-induced STAT1 phosphorylation, the decrease in IL-4-induced STAT6 phosphorylation is in agreement with the previously reported repression of STAT6 activity

upon STAT1 activation[46,47]. We next evaluated the expression of several STAT1 target genes (*Nos2,* Acod1 and Ifit1) in IL-33-treated WT and A20-deficient BMDMs. In agreement with the observed increase in STAT1 phosphorylation, IL-33 stimulation also induced STAT1-dependent gene expression, which was again higher in A20 $^{LysM\text{-}KO}$ BMDMs, especially when cells were pre-stimulated with IL-4 (Fig 4D). Altogether, our data demonstrate that A20 deficiency sensitizes BMDMs to IL-33-induced STAT1 signalling, which is further enhanced by IL-4 co-stimulation and associated with repression of IL-4-induced STAT6 signalling.

A20-deficient macrophages produce IFN-γ in response to IL-33

STAT1 signalling is known to be activated by several cytokines and has been best described as a TF that is activated in several cell types in response to interferons such as IFN-γ[48]. Although IFN-γ is mainly produced by T cells, we also assessed its expression in IL-33-stimulated BMDMs. While WT cells did not produce any IFN-γ in response to IL-33 or IL-33 plus IL-4, IFN-γ expression was drastically increased after 6 h in A20-deficient macrophages and fully dependent on IL-33 stimulation (Fig. 5A).

To further investigate the role of STAT1 in IL-33-induced gene expression in macrophages, we analysed the effect of IL-33 in STAT1-deficient and STAT1/A20-double deficient BMDMs prestimulated with IL-4. STAT1 was indispensable for IL-33-induced expression of *Ifit1*, and at least partially required for IL-33 induced expression of *Acod1, Il1, Il6* and *Nos2* (Fig. 5B). Remarkably, although a role for STAT1 in IFN-γ expression is not known, also IL-33-induced expression of IFN-γ was completely dependent on STAT1 (Fig 5B). Collectively, our data demonstrate a novel and unexpected role for A20 as a

break on IL-33-induced IFN-γ expression in BMDMs, which is shown to be STAT1-dependent.

Increased IFN-γ expression in myeloid cell A20-deficient mice partially mediates the inhibition of type 2 immune responses in IL-33-treated mice

In agreement with our findings that A20-deficient BMDMs start to produce IFN-γ in response to IL-33 treatment *in vitro*, IL-33-treated A20 $^{LysM\text{-}KO}$ mice also showed elevated levels of IFN-γ in lung tissue and in BAL fluid (Fig 5C). Importantly, we also analysed IFN-γ expression specifically in lung interstitial macrophages and detected IFN-γ expression in cells from IL-33-treated A20 $^{LysM\text{-}KO}$ but not A20 $^{LysM\text{-}WT}$ mice (Fig. 5D). IFN-γ has previously been shown to block the proliferation and accumulation of ILC2s in lung tissue and their production of IL-5 in response to IL-33 in a STAT1-dependent manner[49-51]. Therefore, the increased amounts of IFN-γ found in the lung of IL-33-treated A20-deficient mice could potentially explain the reduced number of ILC2s, decreased production of IL-13 and IL-5, and lack of eosinophil infiltration that we found in IL-33-treated A20 $^{LysM\text{-}KO}$ mice compared to WT mice. To further investigate this, we analysed if IL-33 was still able to induce ILC2 and eosinophil expansion in lungs of myeloid A20-deficient mice that we had crossed with full body STAT1-deficient mice. STAT1-deficiency restored ILC2 cell numbers and eosinophilia in response to IL-33 administration in A20 $^{LysM\text{-}KO}$ mice up to 50% of the levels found in A20 $^{LysM\text{-}WT}$ mice, but was not able to completely prevent the effect of A20 deficiency (Fig. 5E). Although we cannot exclude any STAT1-independent effects of IFN-γ, it was previously shown that STAT1 is essential for the inhibition of ILC2 function by IFN-γ[50]. Together these results demonstrate that increased IFN-γ expression

in myeloid cell A20-deficient mice partially mediates the inhibition of type 2 immune responses in IL-33-treated mice.

Discussion

IL-33 is a key cytokine in human lung inflammation (both in asthma and COPD), as well as in atopic dermatitis and food allergy, and several clinical trials with IL-33 or IL-33 receptor targeting monoclonal antibodies are ongoing[29]. A clear understanding of the mechanisms that determine the IL-33 response is therefore of high interest. Our data demonstrate that expression of A20 in myeloid cells determines the immune response to acute IL-33 administration in the lung, shifting it from eosinophilic to more neutrophilic inflammation. While both still result in significant lung damage (with collagen deposition, mucus production), the type of response may have an impact on treatment efficiency (e.g. anti-IL4/13, anti-IgE, anti-IL-33). Importantly, multiple gene polymorphisms in A20 as well as A20 haploinsufficiency have been associated with inflammatory disease development in humans[7,8]. Although A20 haploinsufficiency will lead to more severe inflammatory disease beyond lung inflammation, one could speculate that less drastic differences in A20 expression and/or function in macrophages (e.g. mediated by A20 phosphorylation) may similarly have an impact on the lung inflammatory response. Therefore, our findings may eventually help to identify strategies that allow a better stratification of patients based on functional A20 expression and clinical phenotypes, leading to personalized treatment and enhanced efficacy.

IL-33 is generally considered to promote anti-inflammatory macrophage polarization via induction of type 2 cytokines (IL-4, IL-13), as well as via a direct effect on macrophages primed with IL-4/IL-13[39]. Our data show that IL-33 also induces a typical pro-inflammatory gene profile, which is consistent with another recent report, showing also that weak expression of the anti-inflammatory genes *Arg1*, *Retnla* and *Chil3* was only detectable

upon prolonged IL-33 stimulation (5 days) and mediated via an indirect effect of IL-33 signalling on GATA3 activation[42]. Macrophages in the airways of IL-33-treated myeloid cell A20-deficient mice showed strongly reduced expression of several genes that are also known to be produced by IL-4-activated macrophages, making it likely that many of the observed differences in gene expression in IL-33-treated mice reflect the much lower amounts of IL-4 in the lung environment of IL-33-treated A20 $^{LysM\text{-}KO}$ mice. However, as IL-4 signalling itself is not regulated by A20, we hypothesize that decreased ILC2 expansion and eosinophilia in IL-33-treated myeloid cell A20-deficient mice reflects at least partially a direct effect of A20 on IL-33 signalling in interstitial macrophages.

A20 is mainly known as an anti-inflammatory protein, whose absence in mice or humans is associated with inflammatory disease development[52]. In this context, A20 $^{LysM\text{-}KO}$ mice that were used in the present study have previously been shown to spontaneously develop arthritis[31] and enthesitis[44]. It is now well accepted that A20 exerts its anti-inflammatory function by negatively regulating NF-κB and p38/JNK MAPKs activation in response to TNF and TLR4 stimulation[5]. In agreement with this prevailing paradigm, we could demonstrate that A20 also inhibits IL-33-induced NF-κB and MAPKs activation upon overexpression in HEK293T cells. Furthermore, although A20 deficiency in BMDMs only slightly increased IL-33-induced NF-κB activation, IL-33induced expression of several NF-κB-dependent pro-inflammatory genes was strongly increased in the absence of A20. Most likely this reflects their regulation, directly or indirectly, by other transcription factors whose activity is also downregulated by A20. Unexpectedly, we found that lack of A20 sensitises BMDMs to IL-33-induced STAT1 activation, which was even more pronounced in the presence of IL-4 and also associated with a decrease in IL-4-induced STAT6

activation. The increased IL-33 response in the presence of IL-4 is in line with IL-33 receptor upregulation in response to IL-4Ra signalling[39]. Moreover, as IL-4 is also present in the lung environment of IL-33 treated mice, these *in vitro* conditions can also be expected to be relevant *in vivo*. An IL-33-ST2-MyD88-STAT1 axis has been previously described in IL-33-induced DC maturation[53]. However, in this previous work, STAT1 phosphorylation was measured only after 24 hours of IL-33 stimulation and therefore one cannot exclude that STAT1 activation is secondary to IL-33-induced gene expression. Also, in our study, STAT1 phosphorylation in BMDMs only becomes most detectable at 24 hours after IL-33 plus IL-4 stimulation, although a weak effect can already be observed at 3 hours. This delayed response suggests that IL-33 may also activate STAT1 indirectly by upregulating other STAT1-activating cytokines, such as autocrine type I IFN, IL-12 or others. In principle, the specific role of different cytokines could be analysed further by studying the effect of neutralizing anti-receptor antibodies. However, given the vast amount of other candidate cytokines that should also be excluded, the indirect effect was not further addressed in the current study. In this context, we also made the surprising finding that IL-33 stimulation of A20-deficient BMDMs strongly and rapidly upregulates IFN-γ, which is a major activator of STAT1 signalling. Similarly, IFN-γ expression could be demonstrated in interstitial macrophages isolated from lung of IL-33 treated A20 $^{LysM\text{-}KO}$ mice. Although IFN-γ is mainly produced by T cells and NK cells, macrophages are better known as IFN-γ-responding rather than IFN-γ-producing cells, prior studies have demonstrated that macrophages can secrete IFN-γ under certain conditions[54,55]. This raises the intriguing question how IL-33 activates IFN-γ expression in macrophages. Another member of IL-1 family cytokine, IL-18, was previously shown to induce IFN-γ

expression in the human myelomonocytic cell line KG-1 in an NF-κB-dependent manner[56]. Other transcription factors, such as cAMP response element binding protein (CREB), activating transcription factor 2 (ATF2) and activator protein (AP)-1 have been implicated in the regulation of IFN-γ expression in T cells[57]. Of note, both ATF2 and AP1 were strongly upregulated in A20 $^{LysM\text{-}KO}$ BMDMs stimulated with IL-4 plus IL-33, suggesting that these TFs may also be involved in the regulation of IFN-γ expression in macrophages.

To our big surprise, IL-33-induced IFN-γ expression in A20-deficient BMDMs was found to be completely dependent on STAT1. While STAT1 is well known to be activated by IFN-γ, a role for STAT1 in IFN- γ expression has not yet been described. Only STAT4 has been implicated in IL-12-induced IFN-γ expression[58], but whether STAT4 contributes directly to IFN-γ gene regulation remains controversial, although potential STAT4 binding sites have been reported in the first intron and promoter of the IFN-γ gene[59,60]. It is possible that under certain conditions STAT1 is capable of inducing IFN-γ expression either directly or via induction of T-bet expression[61]. Alternatively, STAT1 is known to form a heterodimer with STAT2 and STAT3, as well as STAT4[62]. However, we did not detect any significant changes in STAT3, STAT4 or STAT5 activity in the transcription factor profiling assay, suggesting a more direct role of STAT1. Because IFN-γ is itself a strong activator of STAT1, a minor upregulation of IFN-γ in macrophages in response to IL-33 can also be expected to be rapidly amplified via a feed-forward loop of STAT1-dependent IFN-γ expression. *In vivo*, the underlying mechanism may be even more complex as other cell types may also contribute to increased IFN-γ. In this context, it was demonstrated that loss of A20 in conventional type 1 DCs led to increased production of the type 2-

suppresive cytokine IL-12 by DCs, which in turn induced IFN-γ production by $CD8^+$ T cells[4]. In conclusion, our findings reveal a novel role for A20 as a negative regulator of STAT1-dependent IFN-γ expression in IL-33-stimulated macrophages. How STAT1 is involved in IL-33-mediated IFN-γ production in macrophages, as well as the mechanism of action of A20, still needs to be clarified.

Our finding that A20 deficiency in myeloid cells results in increased IFN-γ production in response to IL-33 *in vitro* and *in vivo* may have important implications in the regulation of type 1 and type 2 immune responses in the lung and other organs. In this context, several reports point to the existence of a supportive signal supplemented by myeloid cells that facilitate IL-33-induced ILC2 proliferation. Indeed, it has been previously shown that myeloid cell-specific deletion of von Hippel–Lindau (VHL) E3 ligase results in attenuated eosinophilia and reduced ILC2 function in response to papain challenge in a mouse model, which was mechanistically explained by the ability of alveolar macrophages to support IL-33-induced ILC2 proliferation via osteopontin[63]. Similarly, lung ILC2 activation and eosinophilia triggered by *Alternaria alternata* were significantly reduced in mice lacking group V phospholipase A2 (Pla2g5), which was restored by adoptive transfer of wild type BMDM[64]. On the other hand, the here described increased production of IFN-γ by macrophages in A20 $^{LysM\text{-}KO}$ mice might negatively affect ILC2 function. Indeed, IFN-γ is known as a potent repressor of ILC2 activation, proliferation, and type 2 cytokine production[49,50,51]. Consistent with this, we found that defective IL-33-induced ILC2 expansion and eosinophilia in the lungs of mice lacking A20 in myeloid cells was partially rescued by the absence of STAT1, suggesting that the increased IFN-γ production by A20-deficient macrophages plays an important role in the blunting of an IL-33-induced

type 2 immune response in A20 $^{LysM\text{-}KO}$ mice. Because absence of STAT1 also impacts the activity of other cytokines than IFN-γ, we cannot exclude a role for additional cytokines that are produced by myeloid cells and which have also been shown to control ILC2 function, such as IL-27[51].

Together, the here described mechanisms that regulate macrophage function in response to IL-33 might be critical for a better understanding of type 1 and type 2 immune responses that are mediated by IL-33 during infection and allergic inflammation, and may eventually lead to improved therapeutic strategies.

Acknowledgements

We are grateful to Prof. Geert van Loo for providing the myeloid cell-specific A20 knockout (A20LysM-KO) mice, the VIB Protein Core facility for the production and purification of IL-33trap and the VIB Flow Core for assistance with flow cytometry. Marnik Vuylsteke gave advice for statistical analysis. We also thank Dr. Harald Braun for the generation of IL-33trap and Dr. Anne-Marie Pauwels and Dr. Lynn Verstrepen for experimental assistance and useful discussion.

Authors contribution

A.H., C.M., Z.L, C.L.S., I.S.A. and R.B. conceived and designed the experiments. A.H., C.M., I.S.A., M.H., Y.D., M.K., Z.L. and A.A. performed the experiments. A.H., Z.L., C.L.S., I.S.A. and R.B. analysed the data, interpreted the results and wrote the manuscript.

References

1 Hammad H, Lambrecht BN. The basic immunology of asthma. *Cell* 2021; **184**: 1469–1485.

2 Hinks TSC, Levine SJ, Brusselle GG. Treatment options in type-2 low asthma. *Eur Respir J* 2021; **57**: 2000528.

3 Vroman H, Bergen IM, van Hulst JAC, van Nimwegen M, van Uden D, Schuijs MJ *et al.* TNF-α–induced protein 3 levels in lung dendritic cells instruct TH2 or TH17 cell differentiation in eosinophilic or neutrophilic asthma. *J Allergy Clin Immunol* 2018; **141**: 1620-1633.e12.

4 Vroman H, Uden D van, Bergen IM, van Hulst JAC, Lukkes M, van Loo G *et al.* Tnfaip3 expression in pulmonary conventional type 1 Langerin-expressing dendritic cells regulates T helper 2-mediated airway inflammation in mice. *Allergy* 2020; **75**: 2587–2598.

5 Afonina IS, Zhong Z, Karin M, Beyaert R. Limiting inflammation—the negative regulation of NF-κB and the NLRP3 inflammasome. *Nat Immunol* 2017; **18**: 861–869.

6 Schuijs MJ, Willart MA, Vergote K, Gras D, Deswarte K, Ege MJ *et al.* Farm dust and endotoxin protect against allergy through A20 induction in lung epithelial cells. *Science* 2015; **349**: 1106–1110.

7 Stein MM, Hrusch CL, Gozdz J, Igartua C, Pivniouk V, Murray SE *et al.* Innate Immunity and Asthma Risk in Amish and Hutterite Farm Children. *N Engl J Med* 2016; **375**: 411–421.

8 Li X, Ampleford EJ, Howard TD, Moore WC, Torgerson DG, Li H *et al.* Genome-wide association studies of asthma indicate opposite immunopathogenesis direction from autoimmune diseases. *J Allergy Clin Immunol* 2012; **130**: 861-868.e7.

9 Krusche J, Twardziok M, Rehbach K, Böck A, Tsang MS, Schröder PC *et al.* TNF-α-induced protein 3 is a key player in childhood asthma development and environment-mediated protection. *J Allergy Clin Immunol* 2019; **144**: 1684-1696.e12.

10 Heger K, Fierens K, Vahl JC, Aszodi A, Peschke K, Schenten D *et al.* A20-Deficient Mast Cells Exacerbate Inflammatory Responses In Vivo. *PLOS Biology* 2014; **12**: e1001762.

11 Vroman H, Das T, Bergen IM, van Hulst JAC, Ahmadi F, van Loo G *et al.* House dust mite-driven neutrophilic airway inflammation in mice with TNFAIP3-deficient myeloid cells is IL-17-independent. *J Allergy Clin Immunol* 2018; **48**: 1705-1714.

12 Kool M, van Loo G, Waelput W, De Prijck S, Muskens F, Sze M *et al.* The Ubiquitin-Editing Protein A20 Prevents Dendritic Cell Activation, Recognition of Apoptotic Cells, and Systemic Autoimmunity. *Immunity* 2011; **35**: 82–96.

13 Cayrol C. IL-33, an Alarmin of the IL-1 Family Involved in Allergic and Non Allergic Inflammation: Focus on the Mechanisms of Regulation of Its Activity. *Cells* 2022; **11**: 107.

14 Chan BCL, Lam CWK, Tam L-S, Wong CK. IL33: Roles in Allergic Inflammation and Therapeutic Perspectives. *Front Immunol* 2019; **10**: 364.

15 Moffatt MF, Gut IG, Demenais F, Strachan DP, Bouzigon E, Heath S *et al.* A large-scale, consortium-based genomewide association study of asthma. *N Engl J Med* 2010; **363**: 1211–1221.

16 Bønnelykke K, Sleiman P, Nielsen K, Kreiner-Møller E, Mercader JM, Belgrave D *et al.* A genome-wide association study identifies CDHR3 as a susceptibility locus for early childhood asthma with severe exacerbations. *Nat Genet* 2014; **46**: 51–55.

17 Torgerson DG, Ampleford EJ, Chiu GY, Gauderman WJ, Gignoux CR, Graves PE *et al.* Meta-analysis of genome-wide association studies of asthma in ethnically diverse North American populations. *Nat Genet* 2011; **43**: 887–892.

18 Préfontaine D, Nadigel J, Chouiali F, Audusseau S, Semlali A, Chakir J *et al.* Increased IL-33 expression by epithelial cells in bronchial asthma. *J Allergy Clin Immunol* 2010; **125**: 752–754.

19 Hamzaoui A, Berraies A, Kaabachi W, Haifa M, Ammar J, Kamel H. Induced sputum levels of IL-33 and soluble ST2 in young asthmatic children. *J Asthma* 2013; **50**: 803–809.

20 Momen T, Ahanchian H, Reisi M, Shamsdin SA, Shahsanai A, Keivanfar M. Comparison of Interleukin-33 Serum Levels in Asthmatic Patients with a Control Group and Relation with the Severity of the Disease. *Int J Prev Med* 2017; **8**: 65.

21 Kaur D, Gomez E, Doe C, Berair R, Woodman L, Saunders R *et al.* IL-33 drives airway hyper-responsiveness through IL-13-mediated mast cell: airway smooth muscle crosstalk. *Allergy* 2015; **70**: 556–567.

22 Willart MAM, Deswarte K, Pouliot P, Braun H, Beyaert R, Lambrecht BN, Hammad H. Interleukin-1α controls allergic sensitization to inhaled house dust mite via the epithelial release of GM-CSF and IL-33. *J Exp Med* 2012; **209**: 1505–1517.

23 Yin H, Li XY, Liu T, Yuan BH, Zhang BB, Hu SL *et al.* Adenovirus-mediated delivery of soluble ST2 attenuates ovalbumin-induced allergic asthma in mice. *Clin Exp Immunol* 2012; **170**: 1–9.

24 Lee HY, Rhee CK, Kang JY, Byun JH, Choi JY, Kim SJ *et al.* Blockade of IL-33/ST2 ameliorates airway inflammation in a murine model of allergic asthma. *Exp Lung Res* 2014; **40**: 66–76.

25 Chu DK, Llop-Guevara A, Walker TD, Flader K, Goncharova S, Boudreau JE *et al.* IL-33, but not thymic stromal lymphopoietin or IL-25, is central to mite and peanut allergic sensitization. *J Allergy Clin Immunol* 2013; **131**: 187-200.e1–8.

26 Hayakawa H, Hayakawa M, Kume A, Tominaga S. Soluble ST2 blocks interleukin-33 signaling in allergic airway inflammation. *J Biol Chem* 2007; **282**: 26369–26380.

27 Chen W-Y, Tsai T-H, Yang J-L, Li L-C. Therapeutic Strategies for Targeting IL-33/ST2 Signalling for the Treatment of Inflammatory Diseases. *CPB* 2018; **49**: 349–358.

28 Holgado A, Braun H, Van Nuffel E, Detry S, Schuijs MJ, Deswarte K *et al.* IL-33trap is a novel IL-33-neutralizing biologic that inhibits allergic airway inflammation. *J Allergy Clin Immunol* 2019; **144**: 204–215.

29 Morita H, Matsumoto K, Saito H. Biologics for allergic and immunologic diseases. *J Allergy Clin Immunol* 2022; **150**:766-777.

30 Braun H, Afonina IS, Mueller C, Beyaert R. Dichotomous function of IL-33 in health and disease: From biology to clinical implications. *Biochem Pharmacol* 2018; **148**: 238–252.

31 Matmati M, Jacques P, Maelfait J, Verheugen E, Kool M, Sze M *et al.* A20 (TNFAIP3) deficiency in myeloid cells triggers erosive polyarthritis resembling rheumatoid arthritis. *Nat Genet* 2011; **43**: 908–912.

32 Lüthi AU, Cullen SP, McNeela EA, Duriez PJ, Afonina IS, Sheridan C *et al*. Suppression of interleukin-33 bioactivity through proteolysis by apoptotic caspases. *Immunity* 2009; **31**:84-98.

33 Schmitz J, Owyang A, Oldham E, Song Y, Murphy E, McClanahan TK *et al*. IL-33, an interleukin-1-like cytokine that signals via the IL-1 receptor-related protein ST2 and induces T helper type 2-associated cytokines. *Immunity* 2005; **23**:479-90.

34 Wu YH, Lai AC, Chi PY, Thio CL, Chen WY, Tsai CH *et al.* Pulmonary IL-33 orchestrates innate immune cells to mediate respiratory syncytial virus-evoked airway hyperreactivity and eosinophilia. *Allergy* 2020; **75**:818-830.

35 Liegeois M, Legrand C, Desmet CJ, Marichal T, Bureau F. The interstitial macrophage: A long-neglected piece in the puzzle of lung immunity. *Cell Immunol* 2018; **330**: 91-96.

36 Sabatel C, Radermecker C, Fievez L, Paulissen G, Chakarov S, Fernandes C *et al.* Exposure to Bacterial CpG DNA Protects from Airway Allergic Inflammation by Expanding Regulatory Lung Interstitial Macrophages. *Immunity* 2017; **46**: 457–473.

37 Nahrendorf M, Swirski FK. Abandoning M1/M2 for a Network Model of Macrophage Function. *Circ Res* 2016; **119**: 414–417.

38 Wang Q, Hong L, Chen M, Shi J, Lin X, Huang L *et al.* Targeting M2 Macrophages Alleviates Airway Inflammation and Remodeling in Asthmatic Mice via miR-378a-3p/GRB2 Pathway. *Front Mol Biosci* 2021; **8**: 886.

39 Kurowska-Stolarska M, Stolarski B, Kewin P, Murphy G, Corrigan CJ, Ying S *et al.* IL-33 amplifies the polarization of alternatively activated macrophages that contribute to airway inflammation. *J Immunol* 2009; **183**: 6469–6477.

40 Verhelst K, Carpentier I, Kreike M, Meloni L, Verstrepen L, Kensche T *et al.* A20 inhibits LUBAC-mediated NF-κB activation by binding linear polyubiquitin chains via its zinc finger 7. *EMBO J* 2012; **31**: 3845–3855.

41 Hutti JE, Turk BE, Asara JM, Ma A, Cantley LC, Abbott DW. IkappaB kinase beta phosphorylates the K63 deubiquitinase A20 to cause feedback inhibition of the NF-kappaB pathway. *Mol Cell Biol* 2007; **27**: 7451–7461.

42 Faas M, Ipseiz N, Ackermann J, Culemann S, Grüneboom A, Schröder F *et al.* IL-33-induced metabolic reprogramming controls the differentiation of alternatively activated macrophages and the resolution of inflammation. *Immunity* 2021; **54**: 2531-2546.e5.

43 Piccolo V, Curina A, Genua M, Ghisletti S, Simonatto M, Sabò A *et al.* Opposing macrophage polarization programs show extensive epigenomic and transcriptional cross-talk. *Nat Immunol* 2017; **18**: 530-540.

44 De Wilde K, Martens A, Lambrecht S, Jacques P, Drennan MB, Debusschere K *et al.* A20 inhibition of STAT1 expression in myeloid cells: a novel endogenous regulatory mechanism preventing development of enthesitis. *Ann Rheum Dis* 2017; **76**: 585–592.

45 Li J, Shen D, Tang J, Wang Y, Wang B, Xiao Y *et al.* IL33 attenuates ventricular remodeling after myocardial infarction through inducing alternatively activated macrophages ethical standards statement. *Eur J Pharmacol* 2019; **854**:307-319.

46 Ohmori Y, Hamilton TA. Interleukin-4/STAT6 Represses STAT1 and NF-κB-dependent Transcription through Distinct Mechanisms. *J Biol Chem* 2000; **275**: 38095–38103.

47 Venkataraman C, Leung S, Salvekar A, Mano H, Schindler U. Repression of IL-4-induced gene expression by IFN-gamma requires Stat1 activation. *J Immunol* 1999; **162**: 4053–4061.

48 Liu S, Imani S, Deng Y, Pathak JL, Wen Q, Chen Y *et al.* Targeting IFN/STAT1 Pathway as a Promising Strategy to Overcome Radioresistance. *Onco Targets Ther* 2020; **13**: 6037–6050.

49 Molofsky AB, Van Gool F, Liang H-E, Van Dyken SJ, Nussbaum JC, Lee J *et al.* Interleukin-33 and Interferon-γ Counter-Regulate Group 2 Innate Lymphoid Cell Activation during Immune Perturbation. *Immunity* 2015; **43**: 161–174.

50 Duerr CU, McCarthy CDA, Mindt BC, Rubio M, Meli AP, Pothlichet J *et al.* Type I interferon restricts type 2 immunopathology through the regulation of group 2 innate lymphoid cells. *Nat Immunol* 2016; **17**: 65–75.

51 Moro K, Kabata H, Tanabe M, Koga S, Takeno N, Mochizuki M *et al.* Interferon and IL-27 antagonize the function of group 2 innate lymphoid cells and type 2 innate immune responses. *Nat Immunol* 2016; **17**: 76–86.

52 Martens A, van Loo G. A20 at the Crossroads of Cell Death, Inflammation, and Autoimmunity. *Cold Spring Harb Perspect Biol* 2020; **12**: a036418.

53 Dominguez D, Ye C, Geng Z, Chen S, Fan J, Qin L *et al.* Exogenous IL-33 Restores Dendritic Cell Activation and Maturation in Established Cancer. *J Immunol* 2017; **198**: 1365–1375.

54 Munder M, Mallo M, Eichmann K, Modolell M. Murine Macrophages Secrete Interferon γ upon Combined Stimulation with Interleukin (IL)-12 and IL-18: A Novel Pathway of Autocrine Macrophage Activation. *J Exp Med* 1998; **187**: 2103–2108.

55 Bogdan C, Schleicher U. Production of interferon-γ by myeloid cells – fact or fancy? *Trends Immunol* 2006; **27**: 282–290.

56 Kojima H, Aizawa Y, Yanai Y, Nagaoka K, Takeuchi M, Ohta T *et al.* An essential role for NF-kappa B in IL-18-induced IFN-gamma expression in KG-1 cells. *J Immunol* 1999; **162**: 5063–5069.

57 Samten B, Townsend JC, Weis SE, Bhoumik A, Klucar P, Shams H *et al.* CREB, ATF, and AP-1 transcription factors regulate IFN-gamma secretion by human T cells in response to mycobacterial antigen. *J Immunol* 2008; **181**: 2056–2064.

58 Thierfelder WE, van Deursen JM, Yamamoto K, Tripp RA, Sarawar SR, Carson RT *et al.* Requirement for Stat4 in interleukin-12-mediated responses of natural killer and T cells. *Nature* 1996; **382**: 171–174.

59 Xu X, Sun YL, Hoey T. Cooperative DNA binding and sequence-selective recognition conferred by the STAT amino-terminal domain. *Science* 1996; **273**: 794–797.

60 Barbulescu K, Becker C, Schlaak JF, Schmitt E, Meyer zum Büschenfelde KH, Neurath MF. IL-12 and IL-18 differentially regulate the transcriptional activity of the human IFN-gamma promoter in primary CD4+ T lymphocytes. *J Immunol* 1998; **160**: 3642–3647.

61 Kamiya S, Owaki T, Morishima N, Fukai F, Mizuguchi J, Yoshimoto T. An indispensable role for STAT1 in IL-27-induced T-bet expression but not proliferation of naive CD4+ T cells. *J Immunol* 2004; **173**: 3871–3877.

62 Collison LW, Delgoffe GM, Guy CS, Vignali KM, Chaturvedi V, Fairweather D *et al.* The composition and signaling of the IL-35 receptor are unconventional. *Nat Immunol* 2012; **13**: 290–299.

63 Zhang W, Li Q, Li D, Li J, Aki D, Liu Y-C. The E3 ligase VHL controls alveolar macrophage function via metabolic-epigenetic regulation. *J Exp Med* 2018; **215**: 3180–3193.

64 Yamaguchi M, Samuchiwal SK, Quehenberger O, Boyce JA, Balestrieri B. Macrophages regulate lung ILC2 activation via Pla2g5-dependent mechanisms. *Mucosal Immunol* 2018; **11**: 615–626.

Figure legends

Figure 1. Myeloid A20 determines IL-33-induced responses in the lung. A20 $^{LysM\text{-}WT}$ and A20 $^{LysM\text{-}KO}$ mice were injected i.t. for 5 consecutive days with PBS or 1 μg mouse IL-33, as indicated. **A,** Representative hematoxylin and eosin (left, scale bar represents 50 μm), combined AB-PAS mucus staining (middle, scale bar represents 200 μm) and Masson's trichrome collagen staining (right, scale bar represents 200 μm) of lung tissue sections. **B** and **C**, Total cell numbers and individual cell types in BAL fluid (B) (PBS A20 $^{LysM\text{-}WT}$ n=5, PBS A20 $^{LysM\text{-}KO}$ n=5, IL-33 A20 $^{LysM\text{-}WT}$ n=7, IL-33 A20 $^{LysM\text{-}KO}$ n=7) and lung tissue (C) (PBS A20 $^{LysM\text{-}WT}$ n=5, PBS A20 $^{LysM\text{-}KO}$ n=5, IL-33 A20 $^{LysM\text{-}WT}$ n=4, IL-33 A20 $^{LysM\text{-}KO}$ n=5) were identified by means of flow cytometry. **D**, Cytokine concentrations in lung homogenate were measured by means of ELISA. Results are representative of 1(A, C) or 2 independent (B, D) experiments. **E**, Gene expression in sorted CD4+ T cells was measured by qRT-PCR (PBS A20 $^{LysM\text{-}WT}$ n=5, PBS A20 $^{LysM\text{-}KO}$ n=5, IL-33 A20 $^{LysM\text{-}WT}$ n=4, IL-33 A20 $^{LysM\text{-}KO}$ n=5). Each symbol represents one mouse. *Error bars* represent means ± SEs. P-values were determined on log-transformed data using two-way ANOVA with Sidak correction for multiple comparisons (*P < .05, **P < .01, and ***P < .001).

Figure 2. A20-deficient airway macrophages show reduced gene expression in IL-33-treated mice. A20 $^{LysM\text{-}WT}$ and A20 $^{LysM\text{-}KO}$ mice were injected i.t. for 5 consecutive days with PBS or 1 μg mouse IL-33, as indicated (PBS A20 $^{LysM\text{-}WT}$ n=5, PBS A20 $^{LysM\text{-}KO}$ n=5, IL-33 A20 $^{LysM\text{-}WT}$ n=7, IL-33 A20 $^{LysM\text{-}KO}$ n=7). **A,**, Gene expression in lung homogenates was measured by qRT-PCR. **B**, *Retnla/Nos2* expression by interstitial macrophages was analysed by qRT-PCR on sorted cells. Results are representative of 2

(A) and 1 (B) independent experiments. Each symbol represents one mouse. *Error bars* represent means ± SEs. P-values were determined on log-transformed data using two-way ANOVA with Sidak correction for multiple comparisons (*P < .05, **P < .01, and ***P < .001).

Figure 3. A20 inhibits IL-33-induced NF-κB and MAPK activation in HEK293T cells but has only a minimal effect in BMDMs. A, HEK293T cells were transfected with IL-33 receptor expression plasmids. Cells were treated with recombinant IL-33, as indicated. IκBα phosphorylation and degradation, as well as p38 and JNK phosphorylation were analyzed by immunoblotting with the antibodies indicated. Actin was used as a loading control. **B** and **C**, HEK293T cells were transfected with NF-κB reporter plasmid, A20 constructs and IL-33 receptor expression plasmids, as indicated. Cells were treated with recombinant IL-33. Luciferase activity in cell lysates was measured 5 hours later and IL-8 secretion in the supernatants was measured by ELISA 24 h later. *Error bars* represent means ± SEs of technical replicates. A20 expression was verified by immunoblotting. **D**, BMDMs were stimulated with IL-33 or LPS, as indicated. IκBα phosphorylation and degradation, as well as p38 and JNK phosphorylation were analysed by immunoblotting with the antibodies indicated. Actin was used as a loading control. Arrowhead indicates position of phosphorylated A20. **E**, BMDMs were left untreated or pre-stimulated with IL-4 for 18 h, followed by IL-33 stimulation for an additional 6 h, as indicated. Gene expression was measured by qRT-PCR. Results are representative of 3 independent experiments. *Error bars* represent means ± SEs of biological (E) replicates. P-values

were determined on log-transformed data using two-way ANOVA with Tukey's correction for multiple comparisons (*P < .05, **P < .01, and ***P < .001).

Figure 4. A20 deficiency sensitizes BMDMs to IL-33-induced STAT1 activation. A and **B**, BMDMs were pre-stimulated with IL-4 for 18 h, followed by IL-33 stimulation for an additional 24 h. Activity of 48 transcription factors was measured in nuclear extracts and reported as relative light units (RLU) in a heatmap **A,** showing relative activity of the indicated transcription factors that exhibited over 2-fold change between samples (GAS/ISRE fold change is shown only in B). **B**, Transcription factors that showed over 4-fold change in their activity. **C,** BMDMs were left untreated or pre-stimulated with IL-4 for 18 h, followed by IL-33 stimulation for 3 h or 24 has indicated. Where indicated IL-33 was pre-incubated with IL-33 inhibitor, IL-33trap. STAT1 and STAT6 phosphorylation were analyzed by immunoblotting with the antibodies indicated. Actin was used as a loading control. Results are representative of two independent experiments. **D,** BMDMs were left untreated or pre-stimulated with IL-4 for 18 h, followed by IL-33 stimulation for 6 h. Gene expression was measured by RT-PCR. Results are representative of 2 independent experiments. *Error bars* represent means ± SEs of biological replicates. P-values were determined on log-transformed data using two-way ANOVA with Tukey's correction for multiple comparisons (*P < .05, **P < .01, and ***P < .001).

Figure 5. IL-33-treated A20-deficient macrophages produce IFN-γ, which partially inhibits IL-33-induced immune responses *in vivo*. A, BMDMs were left untreated or pre-stimulated with IL-4 for 18 h, followed by IL-33 stimulation for 6 h. Gene expression

was measured by qRT-PCR. *Error bars* represent means ± SEs of biological replicates. P-values were determined on log-transformed data using two-way ANOVA with Tukey's correction for multiple comparisons. **B,** BMDMs isolated from A20 $^{LysM\text{-}WT}$ and $^{A20\ LysM\text{-}KO}$ mice, as well as the corresponding mice that were crossed with full body STAT1-deficient mice, were left untreated or pre-stimulated with IL-4 for 18 h, followed by IL-33 stimulation for 6 h. Gene expression was measured by qRT-PCR. P-values were determined using log-linear regression model fitted to the qPCR data of all genes measured simultaneously, as implemented in Genstat software (version 22). The dispersion parameter for the variance of the response was estimated from the residual mean square of the fitted model. T statistics were used to assess the significance of treatment and genotype effects (on the log transformed scale) by pairwise comparisons to A20$^{LysM\text{-}KO}$ IL-33-treated set as reference level. *Error bars* represent means ± SEs of technical replicates. **C**, A20$^{LysM\text{-}WT}$ and A20 $^{LysM\text{-}KO}$ mice were injected i.t. for 5 consecutive days with PBS (n=5) or 1 μg mouse IL-33 (n=7), as indicated. IFN-γ concentrations in lung homogenate and BAL fluid were measured by means of ELISA. P-values were determined using log-linear regression model fitted to the ELISA data measured in both lung and BALF. The dispersion parameter for the variance of the response was estimated from the residual mean square of the fitted model. Wald statistics were used to assess the significance of the main effects genotype and treatment and its interaction term, by dropping these fixed terms from the full model. *Error bars* represent means ± SEs of biological replicates. **D,** *Ifng* gene expression in sorted interstitial macrophages was measured by qRT-PCR (PBS A20 $^{LysM\text{-}WT}$ n=5, PBS A20 $^{LysM\text{-}KO}$ n=5, IL-33 A20 $^{LysM\text{-}WT}$ n=4, IL-33 A20 $^{LysM\text{-}KO}$ n=5). P-value was determined using one-tailed Mann-Whitney U (Wilcoxon rank-sum) test. Based

on the prior knowledge from Fig. 5A-C, we tested the null hypothesis that *Ifng* expression in A20$^{LysM-KO}$ IM is not greater than in A20$^{LysM-WT}$ IM. *Ifng* expression was compared only in IL-33-treated A20$^{LysM-KO}$ and A20$^{LysM-KO}$ groups (all values in both PBS-treated groups were 0). *Error bars* represent means ± SEs of biological replicates. **E,** A20 $^{LysM-WT}$ and ^{A20} $^{LysM-KO}$ mice, as well as the corresponding mice that were crossed with full body STAT1-deficient mice, were injected i.t. for 5 consecutive days with PBS or 1 μg mouse IL-33, as indicated (STAT1 WT: PBS A20 $^{LysM-WT}$ n=4, PBS A20 $^{LysM-KO}$ n=2, IL-33 A20 $^{LysM-WT}$ n=6, IL-33 A20 $^{LysM-KO}$ n=4; STAT1 KO: PBS A20 $^{LysM-WT}$ n=5, PBS A20 $^{LysM-KO}$ n=5, IL-33 A20 $^{LysM-WT}$ n=6, IL-33 A20 $^{LysM-KO}$ n=6). Eosinophil numbers in BAL fluid and ILC2 numbers in lung tissue were identified by means of flow cytometry. Each symbol represents one mouse. *Error bars* represent means ± SEs of biological replicates. P-values were determined on non-transformed (eosinophils) or log-transformed data (ILC2) using two-way ANOVA with Tukey's correction for multiple comparisons (**P* < .05, ***P* < .01, and ****P* < .001).

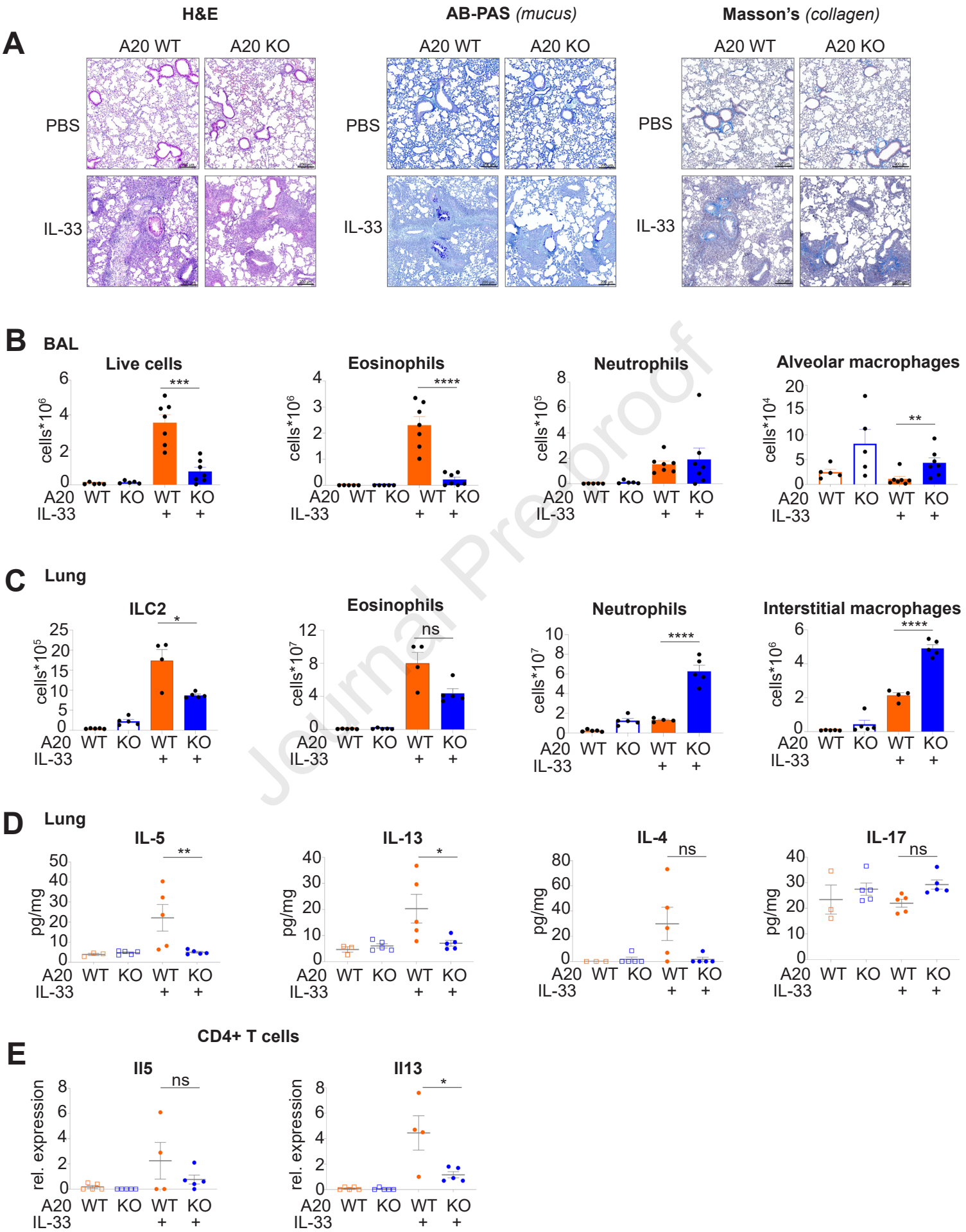

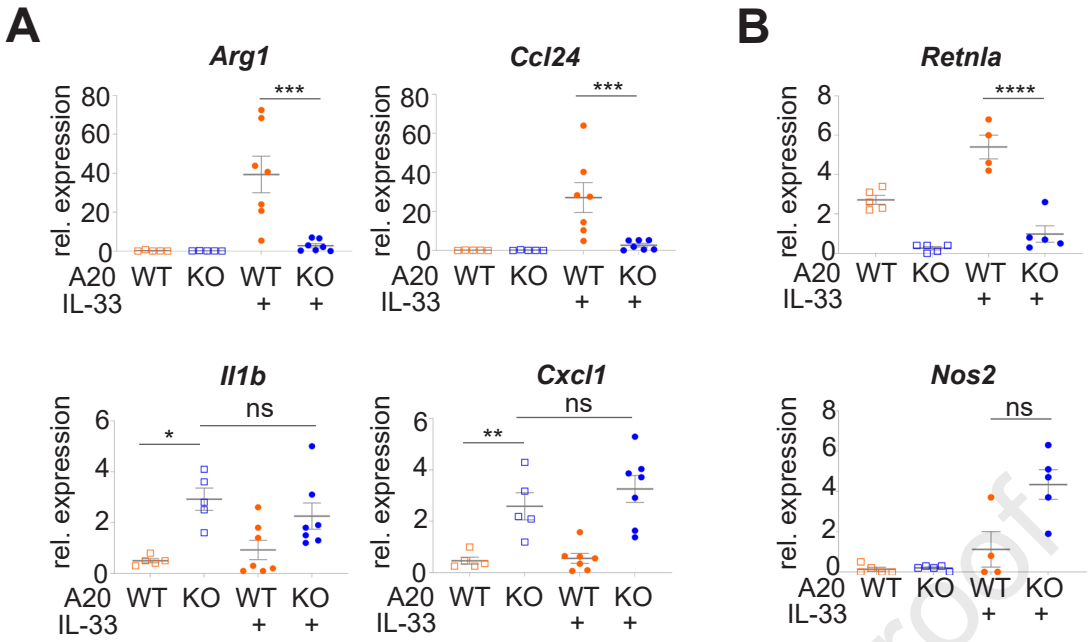

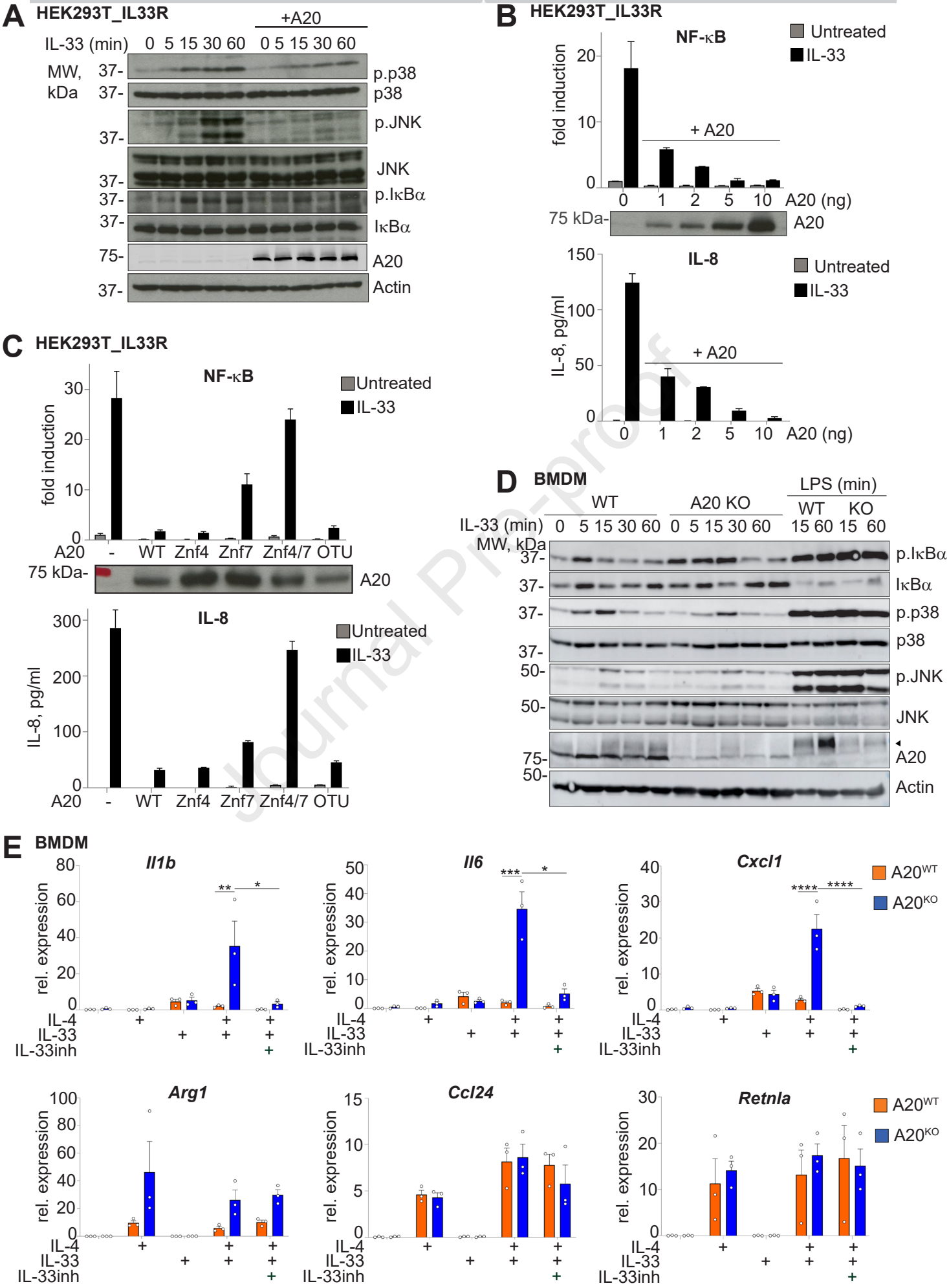

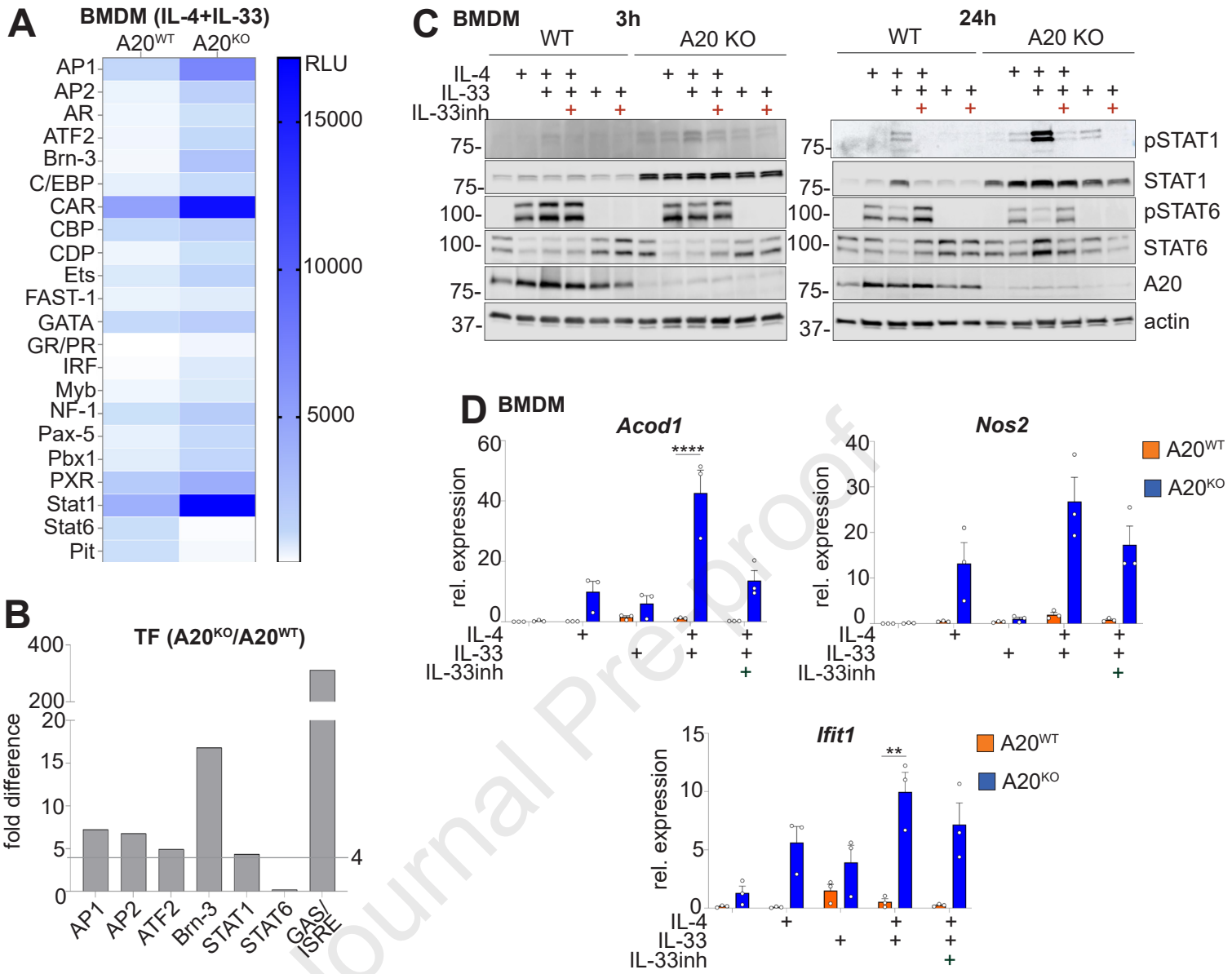

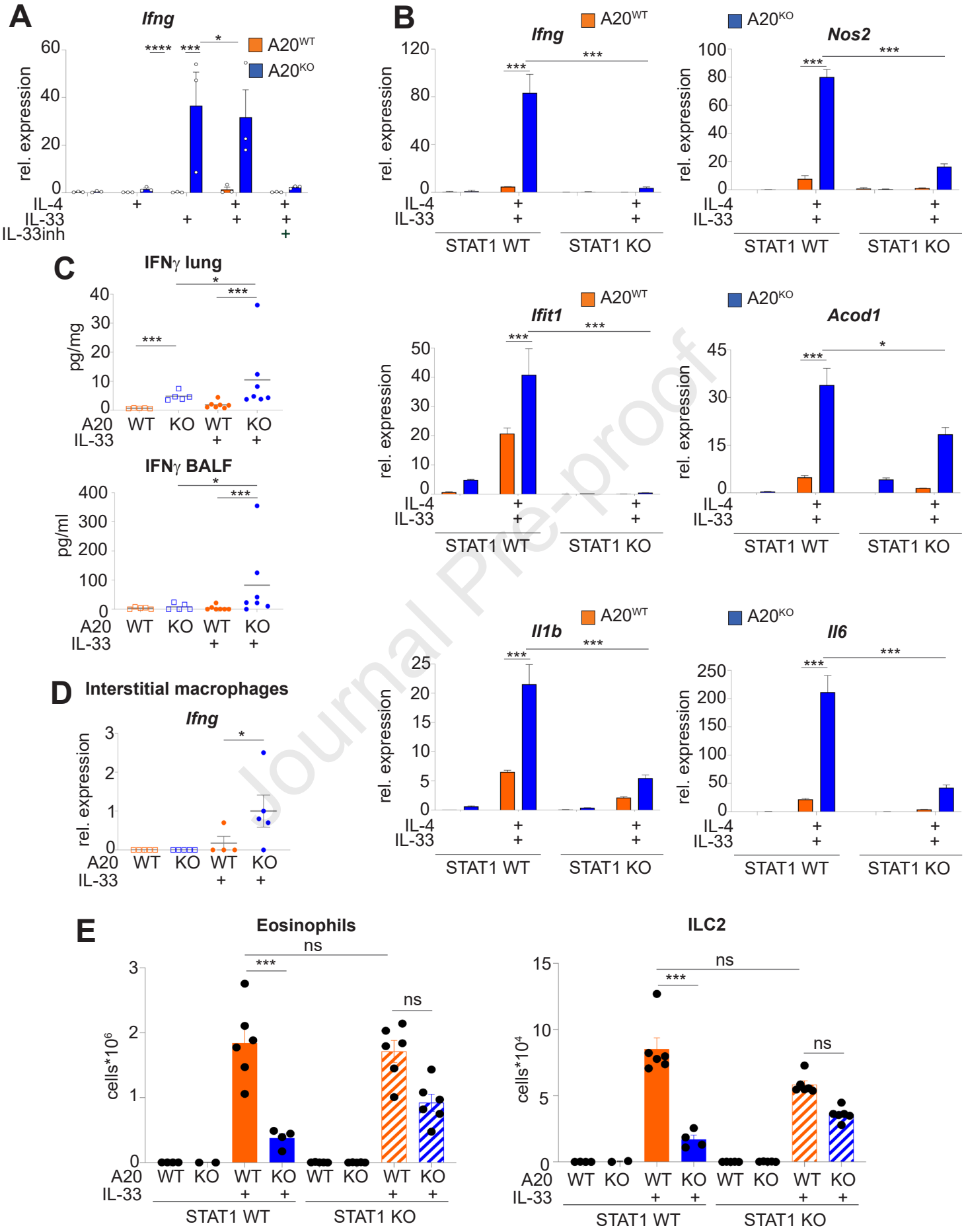

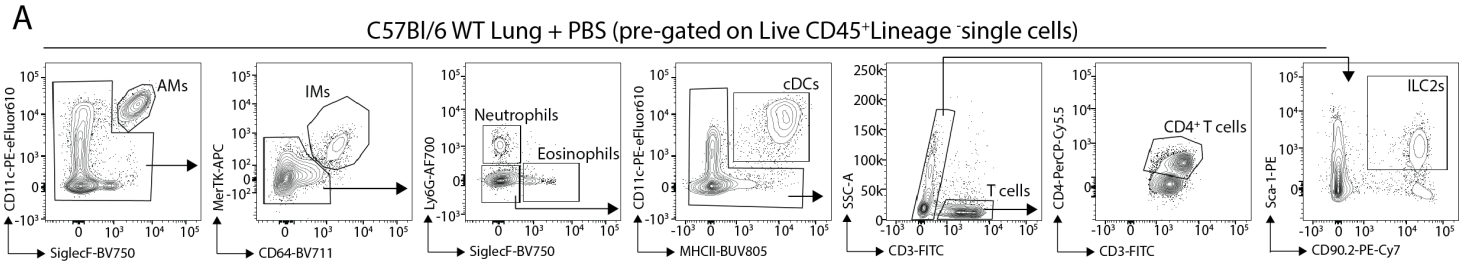

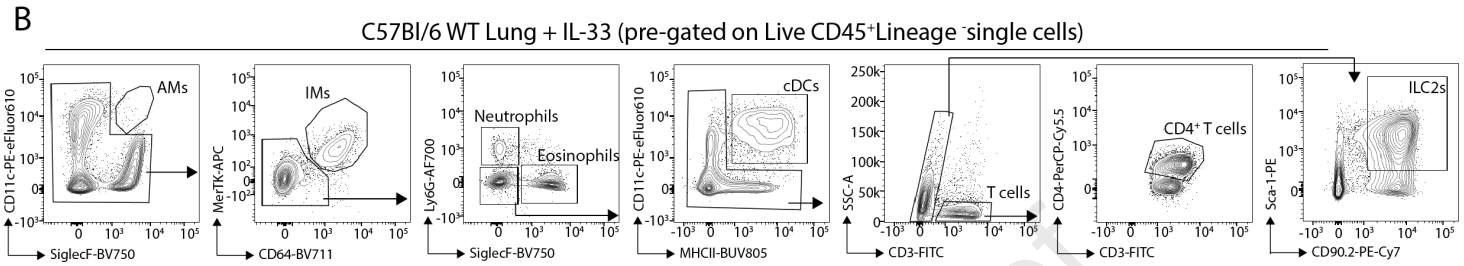

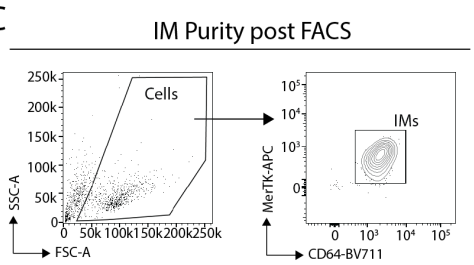

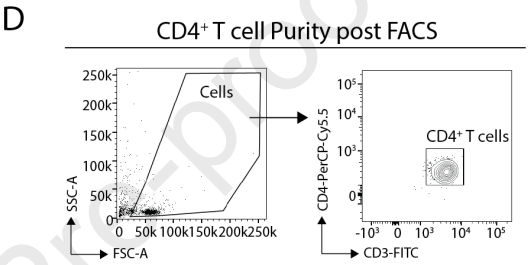

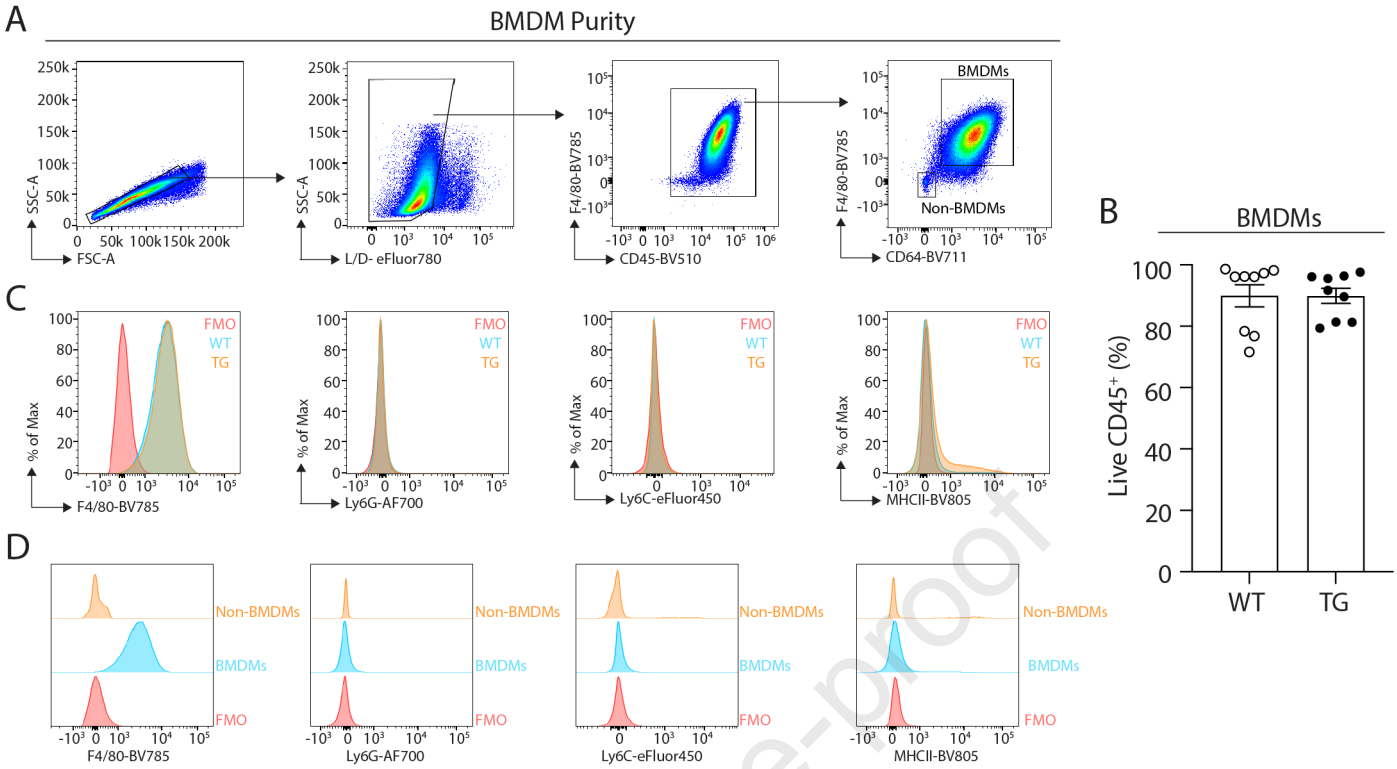

ONLINE REPOSITORY

A20 is a master switch of IL-33 signalling in macrophages and determines IL-33-induced lung immunity

Aurora Holgado MSc[1,2], Zhuangzhuang Liu MSc[2,3], Aigerim Aidarova MSc[1,2], Christina Mueller PhD[1,2], Mira Haegman BSc[1,2], Yasmine Driege BSc[1,2], Marja Kreike BSc[1,2], Charlotte L. Scott PhD[2,3], Inna S. Afonina PhD[1,2*] and Rudi Beyaert PhD[1,2*]

[1]Unit of Molecular Signal Transduction in Inflammation, VIB-UGent Center for Inflammation Research, Ghent, Belgium.

[2]Department of Biomedical Molecular Biology, Ghent University, Ghent, Belgium.

[3]Laboratory of Myeloid Cell Biology in Tissue Damage and Inflammation, VIB-UGent Center for Inflammation Research, Ghent, Belgium.

[*]These authors share senior authorship.

Corresponding author: Rudi Beyaert, PhD, Unit of Molecular Signal Transduction in Inflammation, VIB-UGent Center for Inflammation Research, Ghent, Belgium. E-mail: Rudi.Beyaert@irc.vib-ugent.be

Figure E1. Gating strategies and FACS purities for lung cells. A and B, Representative gating strategy for indicated cell types isolated from lungs of C57Bl/6 WT mice treated for 5 days with PBS (A) or IL-33 (B). AM; Alveolar macrophage, IM; Interstitial macrophage, cDCs; conventional Dendritic cells. The same gating strategy was also applied to the A20 $^{LysM\text{-}KO}$ lungs. **C and D,** Representative post FACS purity checks for IMs and CD4+ T cells. These cells were utilised for qPCR experiments in Figs. 1E, 2B and 5D.

Figure E2. Loss of A20 from LysM-expressing cells has no effect on BMDM purity. Femurs and tibias were removed from A20 $^{LysM\text{-}WT}$ and A20 $^{LysM\text{-}KO}$ mice, BM was isolated and cultured with M-CSF to induce BMDM differentiation. 6 days later purity of the BMDMs was assessed using flow cytometry. **A,** Representative gating strategy used to identify BMDMs. **B,** BMDMs as a proportion of live CD45+ cells in the cultures. Data are pooled from 3 experiments, where each data point indicates a different mouse n= 9 per genotype. ns; student's t test. **C,** Representative histograms showing expression of indicated markers by BMDMs gated as shown in A from WT (cyan) or TG (orange) mice compared with FMO controls (red). **D,** Representative histograms showing expression of indicated markers by BMDMs (cyan) or non-BMDMs (orange) gated as shown in A compared with FMO controls (red). (C,D) Data are representative of 2 experiments with n=6 per genotype.

Table E1. List of antibodies used for flow cytometry, including clone number, dilution used, manufacturer and catalogue number.

Antibody	Clone	Dilution	Figures	Company	Number
B220 FITC	RA3-6B2	400	5D ILC2	BD Biosciences	553087
B220 PE-Cy5	RA3-6B2	300	1C	Biolegend	103202
CD3 PE-Cy5	145-2C11	200	1B, 5D	Tonbo Biosciences	550031
CD3 FITC	145-2C11	100	1C, 5D ILC2	Tonbo Biosciences	350031
CD4 PerCP-Cy5.5	RM4-5	200	1C	Biolegend	100540
CD8a FITC	53-6.7	50	5D ILC2	BD Biosciences	553030
CD11b BUV395	M1/70	200	1C	BD Biosciences	563553
CD11b V450	M1/70	800	1B, 5D eos	BD Biosciences	560455
CD11b FITC	M1/70	200	5D ILC2	ThermoFischer	11-0112-82
CD16/32	2.4G2	400	1,5	BD Biosciences	553142
CD11c PE-Cy7	N418	400	1B	Biolegend	117317
CD11c APC	N418	400	5D eos	ThermoFischer	17-0114
CD11c FITC	HL3	100	5D ILC2	BD Biosciences	553801
CD11c PE-eFluor610	N418	400	1C	ThermoFischer	61-0114-82
CD19 FITC	1D4	800	5D ILC2	Tonbo Biosciences	350193
CD19 PE-Cy5	eBio1D3	400	1B, 5D eos	ThermoFischer	15-0193
CD25 PE-Cy7	PC61.5	400	5D ILC2	ThermoFischer	25-0251-82
CD45 APC	30-F11	800	5D ILC2	Biolegend	103112
CD45 BV510	30-F11	200	1C, S2	Biolegend	103138
CD64 BV711	X54-5/7.1	100	1B, 1C, S2	Biolegend	139311
CD90.2 BV605	30-H12	100	5D ILC2	Biolegend	105343
CD90.2 PE-Cy7	53-2.1	400	1C	Biolegend	140310
CD117 APC-eF780	2B8	150	5D ILC2	ThermoFischer	47-1171-82

CD127 PE-CF594	SB/199	100	5D ILC2	BD Biosciences	562419
F4/80 BV785	BM8	200	S2	Biolegend	123141
Fixable Viability Dye eFluor 506	NA	200	1B, 5D	ThermoFischer	65-0866-18
Fixable Viability Dye eFluor™ 780	NA	500	1C, S2	ThermoFischer	65-0865-14
Ly6C	HK1.4	400	S2	ThermoFischer	48-5932-82
Ly6G AF700	1A8	500	1B, 1C, 5D eos	BD Biosciences	561236
MerTK APC	2B10C42	100	1C	Biolegend	2B10C42
Mer-TK PerCP-eF710	DS5MMER	200	1B	ThermoFischer	46-5751-80
MHC II APC-eFluor780	M5/114.15.2	800	1B	ThermoFischer	47-5321-82
MHCII BUV805	M5/114.15.2	400	1C	BD Biosciences	748844
MHC II FITC	M5/114.15.2	200	5D eos	ThermoFischer	11-5321-85
NK1.1 FITC	PK136	300	5D ILC2	ThermoFischer	11-5941
NK1.1 PE-Cy5	PK136	300	1C	Biolegend	108716
TER-119 PE-Cy5	TER-119	300	1C	ThermoFischer	15-5921-82
TER-119 FITC	TER-119	200	5D ILC2	ThermoFischer	11-5921-85
Sca-1 PE	D7	200	1C	ThermoFischer	12-5981-82
Siglec F PE	E50-2440	1000	1B, 5D eos	BD Biosciences	552126
SiglecF BV750	E50-2440	100	1C	Biolegend	747316
streptavidin BV786	NA	200	5D ILC2	BD Biosciences	563858
ST2 biotin	DJ8	100	5D ILC2	MD Bioproducts	101001B
ST2 BV605	DIH9	100	1C	Biolegend	145323

Table E2. Transcription factor activation profile analysing the activities of 48 TFs. BMDMs were pre-stimulated with IL-4 for 18h, followed by IL-33 stimulation for an additional 24 h. Activity of 48 transcription factors was measured in nuclear extracts and reported as relative light units.

TFs	A20WT	A20KO	TFs	A20WT	A20KO
AP1	977	7081	**NF-1**	469	1800
AP2	218	1479	**NFAT**	638	784
AR	173	459	**NF-E2**	1009	1525
ATF2	169	834	**NFKB**	230	221
Brn-3	146	2455	**4-Oct**	152	254
C/EBP	256	664	**p53**	36	68
CAR	5025	16074	**Pax-5**	250	805
CBF	718	1553	**Pbx1**	298	1049
CDP	187	472	**Pit**	476	140
CREB	233	228	**PPAR**	772	871
E2F-1	531	808	**PXR**	1944	4174
EGR	166	180	**SMAD**	70	74
ER	107	177	**Sp1**	1236	602
Ets	345	1295	**SRF**	474	301
FAST-1	222	304	**SATB1**	135	130
GAS/ISRE	731	228330	**Stat1**	3944	17173
GATA	735	1649	**STAT3**	96	61
GR/PR	61	168	**Stat4**	99	131
HIF	180	330	**Stat5**	84	72
HNF4	397	338	**Stat6**	489	100
IRF	88	331	**TCF/LEF**	5862	7105
MEF2	178	235	**YY1**	795	71
Myb	174	356	**TR**	474	371
Myc/Max	66	119	**TFIID**	311	519